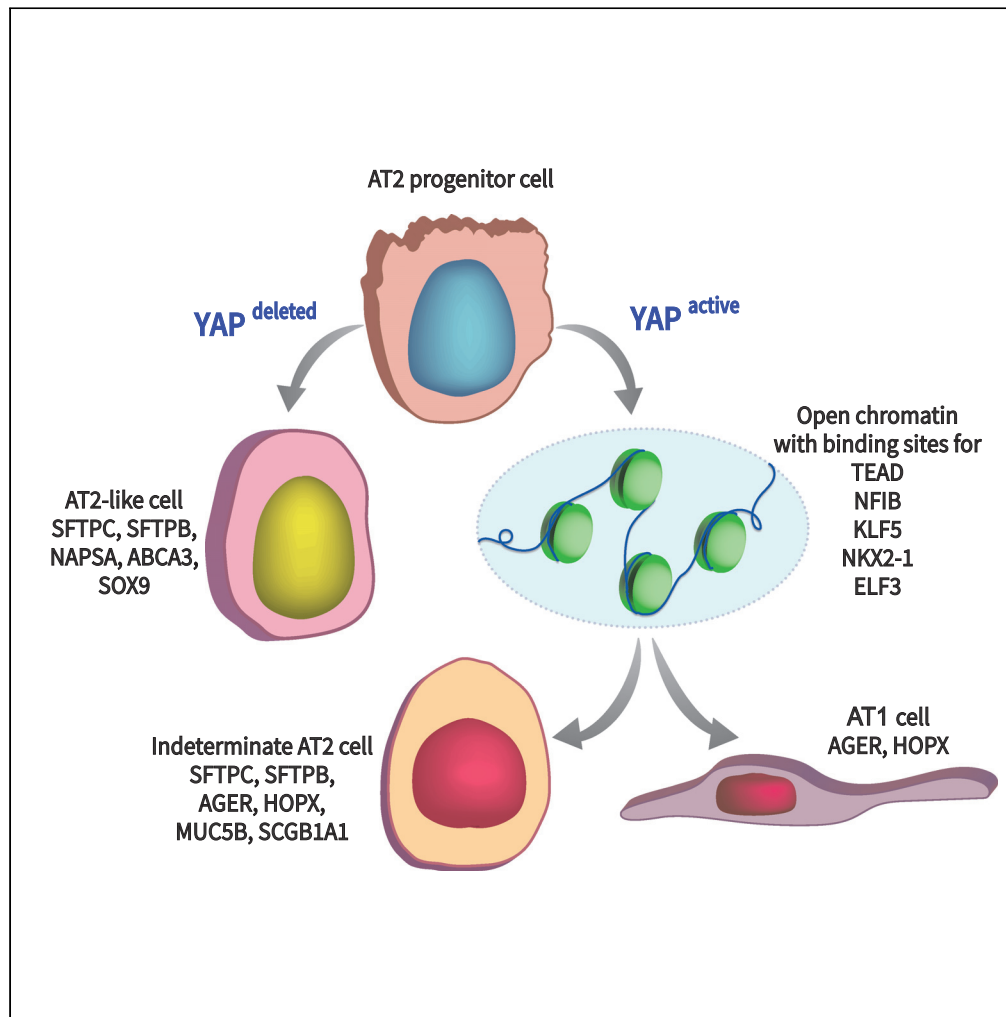


Article

# YAP regulates alveolar epithelial cell differentiation and *AGER* via NFIB/KLF5/NKX2-1



Jason J. Gokey,  
John Snowball,  
Anusha Sridharan,  
Parvathi Sudha,  
Joseph A.  
Kitzmilller, Yan Xu,  
Jeffrey A. Whitsett

jason.j.gokey@vumc.org  
(J.J.G.)  
jeffrey.whitsett@cchmc.org  
(J.A.W.)

**Highlights**

YAP, TEAD, NKX2-1, KLF5 and NFIB interact to increase expression of *AGER*

Active YAP expression induces widespread increased accessibility of chromatin regions

YAP deletion enhances expression of mature AT2 cell markers

YAP activation increases expression of AT1 cell related genes and number of AT1 cells

Gokey et al., iScience 24, 102967  
September 24, 2021 © 2021 The Authors.  
<https://doi.org/10.1016/j.isci.2021.102967>



## Article

YAP regulates alveolar epithelial cell differentiation and *AGER* via NFIB/KLF5/NKX2-1

Jason J. Gokey,<sup>1,5,\*</sup> John Snowball,<sup>2</sup> Anusha Sridharan,<sup>2</sup> Parvathi Sudha,<sup>3</sup> Joseph A. Kitzmiller,<sup>2</sup> Yan Xu,<sup>3,4</sup> and Jeffrey A. Whitsett<sup>2,4,\*</sup>

## SUMMARY

**Ventilation is dependent upon pulmonary alveoli lined by two major epithelial cell types, alveolar type-1 (AT1) and 2 (AT2) cells. AT1 cells mediate gas exchange while AT2 cells synthesize and secrete pulmonary surfactants and serve as progenitor cells which repair the alveoli. We developed transgenic mice in which YAP was activated or deleted to determine its roles in alveolar epithelial cell differentiation. Postnatal YAP activation increased epithelial cell proliferation, increased AT1 cell numbers, and caused indeterminate differentiation of subsets of alveolar cells expressing atypical genes normally restricted to airway epithelial cells. YAP deletion increased expression of genes associated with mature AT2 cells. YAP activation enhanced DNA accessibility in promoters of transcription factors and motif enrichment analysis predicted target genes associated with alveolar cell differentiation. YAP participated with KLF5, NFIB, and NKX2-1 to regulate *AGER*. YAP plays a central role in a transcriptional network that regulates alveolar epithelial differentiation.**

## INTRODUCTION

The respiratory epithelium is formed from embryonic endodermal progenitors that differentiate into a diversity of cell types that vary during development and along the anterior-posterior axis of the lung (Whitsett et al., 2019; Guo et al., 2019). Airways are lined by multiple epithelial cell types including club, goblet, ciliated, ionocytes, tuft, neuroendocrine, and basal cells (Rock et al., 2010; Perl et al., 2002; Rawlins et al., 2007; Cardoso, 2001; Tsao et al., 2009; Reynolds et al., 2002). The alveoli are lined by two major epithelial cell types, alveolar type 1 (AT1) and alveolar type 2 (AT2) cells. AT2 cells secrete surfactant proteins and lipids which serve important roles in innate host defense and in reduction of surface tension at the air/liquid interface. Subsets of AT2 cells also act as progenitor cells, which proliferate to self-renew or differentiate into AT1 cells that are required for efficient gas exchange with endothelial cells of the pulmonary microvasculature (Besnard et al., 2010; Lee et al., 2006; Cutz et al., 2000; Besnard et al., 2009; Bridges et al., 2003; Dahlin et al., 2004; Demling et al., 2006; Kasper et al., 1994; Matsuzaki et al., 2008; Lee et al., 2013; Park et al., 2004; Barkauskas et al., 2013). During lung morphogenesis, Sox9 expressing epithelial cells serve as alveolar progenitors. In the perinatal period, a subset of bi-potent (AT1/AT2) alveolar cells generate mature AT1 or AT2 cells (Rockich et al., 2013; Ustiyani et al., 2016; Guo et al., 2019; Treutlein et al., 2014). While cell turnover and proliferation are not highly active in the mature lung, the lung has a remarkable capacity to repair after injury (Warburton et al., 2001; Vaughan et al., 2015; Zuo et al., 2015; Lechner et al., 2017; Vaughan and Chapman, 2013; Hogan et al., 2014). During regeneration, a subset of Axin2+ AT2 cells act as facultative progenitors of both AT2 and AT1 populations (Zepp et al., 2017; Frank et al., 2016; Zacharias et al., 2018; Nabhan et al., 2018). YAP is dynamically regulated throughout development and regeneration (Isago et al., 2020; Lacanna et al., 2019; Liu et al., 2015; Mahoney et al., 2014; van Soldt et al., 2019), and recent studies demonstrated that Hippo/YAP signaling plays important roles in regulating proliferation and differentiation of both conducting airway and alveolar epithelial cells (Lange et al., 2015; Nantie et al., 2018).

Hippo/YAP signaling plays diverse and important roles in cell proliferation and differentiation to regulate organ size and regeneration. The Hippo/YAP pathway consists of MST1/2 (*Stk4/Stk3*) that direct phosphorylation of LATS. LATS then phosphorylates YAP to direct it to the cytoplasm, where it is sequestered or marked for 14-3-3 ubiquitination and degradation. In the absence of this phosphorylation, YAP is shuttled to the nucleus where it interacts with transcriptional co-factors, including TEADs 1-4, to regulate

<sup>1</sup>Department of Medicine, Division of Allergy, Pulmonary, and Critical Care Medicine, Vanderbilt University Medical Center, Nashville, TN 37232, USA

<sup>2</sup>Division of Neonatology, Perinatal and Pulmonary Biology, Cincinnati Children's Hospital Medical Center, Perinatal Institute, Cincinnati, OH 45229, USA

<sup>3</sup>Division of Biomedical Informatics, Cincinnati Children's Hospital Medical Center, Cincinnati, OH 45229, USA

<sup>4</sup>The Department of Pediatrics, University of Cincinnati College of Medicine, Cincinnati, OH 45229, USA

<sup>5</sup>Lead contact

\*Correspondence:

jason.j.gokey@vumc.org (J.J.G.),

jeffrey.whitsett@cchmc.org (J.A.W.)

<https://doi.org/10.1016/j.isci.2021.102967>



transcription of genes associated with cell proliferation, migration, and differentiation (Varelas, 2014; Yu et al., 2015; Zhao et al., 2011; Pflieger, 2017). YAP interacts with several developmental pathways to regulate cell behaviors (Piersma et al., 2015; van Soldt and Cardoso, 2020), including Wnt signaling to control cell proliferation and differentiation (Gokey et al., 2018). In the developing airway, YAP directs basal cell fate decisions, with both nuclear and cytoplasmic YAP playing independent roles (Mahoney et al., 2014; Lange et al., 2015; Zhao et al., 2014; van Soldt et al., 2019). Activation of YAP in primary human bronchial epithelial cells induced AT1 cell signature genes *HOPX*, *PDPN*, and *AQP5* (Lange et al., 2015). In the embryonic lung, activation of YAP by deletion of *LATS1/2* in AT2 cells increased AT1 cell numbers (Nantie et al., 2018). In idiopathic pulmonary fibrosis, a disease associated with failure of alveolar repair, activated YAP interacts with mTOR to direct cell migration and proliferation, contributing to aberrant gene expression in AT2 cells (Gokey et al., 2018). Although YAP is known to regulate AT1 cell differentiation, the underlying mechanisms remained unclear. Therefore, we sought to identify transcriptional mechanisms by which YAP regulates alveolar epithelial proliferation and differentiation in the postnatal lung.

## RESULTS

To determine the role of epithelial YAP activation or deletion during postnatal alveologenesis, tamoxifen inducible *Sftpc<sup>tm1(cre/ERT2)Blh</sup>* driver was used to constitutively activate YAP by deleting *Stk3<sup>fllox/fllox</sup>/Stk4<sup>fllox/fllox</sup>* (hereafter referred to as YAP<sup>active</sup>) or inhibiting YAP activity by deleting *Yap<sup>fllox/fllox</sup>* (hereafter referred to as YAP<sup>deleted</sup>) (Figure 1A). Tamoxifen injected Cre-negative mice were used as wild type (WT) controls. To study the role of YAP during postnatal alveolar development, mice were exposed to tamoxifen at postnatal day 3 (PND3). Lung immunofluorescence staining, and gene expression were examined at PND14, 28, and 90 (Figure 1). Postnatal activation or inhibition of YAP did not affect survival, in contrast to previous findings, demonstrating embryonic lethality after deletion of *Stk3/Stk4* in mice (Lange et al., 2015). Nuclear localization of YAP was increased in YAP<sup>active</sup> mice. Nuclear YAP was detected in approximately 80% of AT2 cells (Figure 1C) and RNA analysis demonstrated an approximately 90% reduction in *Stk3* and *Stk4* at PND14 (Figures 1B and 1D). Nuclear YAP was detected in 20% of AT2 cells in PND14 WT mice and rarely detected in older WT or YAP<sup>deleted</sup> mice (Figures 1B and 1C). Expression of known YAP transcriptional target genes (e.g., *Ajuba* and *Ctgf*) was decreased in CD45-, CD16/32-, Ter119-, CD90.2-, CD271-, CD31-, EPCAM+ cells (hereafter referred to as EPCAM+ or interchangeably as AT2) isolated from YAP<sup>deleted</sup> mice, consistent with inhibition of YAP activity (Figure 1E). Alveolar spaces were significantly increased ( $P < 0.05$ ) in YAP<sup>deleted</sup> lungs at PND14 and 28. Alveolar spaces in YAP<sup>active</sup> lungs were not different from control lungs (Figure 1F).

### YAP activation and deletion alters the alveolar epithelial cell populations *in vivo*

To identify the role of alveolar epithelial YAP activity during postnatal development, immunofluorescence staining of HOPX, AGER, SFTPC, SFTPB, and Ki67 was assessed in mice at PND14, 28, and 90 (Figure 2). Proliferation of SFTPC+ cells, identified by Ki67+ expression, was increased at PND14 and was sustained thereafter in YAP<sup>active</sup> mice, times at which Ki67+ cells were rarely detected in control mice. Activation of YAP increased numbers of NKX2-1+ SFTPC+SFTPB+ (AT2), and AGER+HOPX+ (AT1) cells (Figures 2A–2C). Along with AT2 and AT1 cells, abnormal alveolar epithelial cell subtypes were identified in YAP<sup>active</sup> mice. Atypical HOPX+AGER+SFTPC+ AT1/AT2 “dual positive” cells were present in YAP<sup>active</sup> lungs that persisted through PND90, perhaps indicating incomplete differentiation (Figure 2D). Atypical AT2 cell doublets of SFTPC+ cells were identified in YAP<sup>active</sup> mice, of which one cell generally exhibited readily detectable Ki67+ staining. These findings are consistent with the concept that YAP activates alveolar progenitor cell proliferation and that increased activity of YAP prevents normal AT2 and AT1 cell differentiation. In contrast, proliferation was significantly decreased at PND14 and the numbers of HOPX+ AT1 and SFTPC+ AT2 cells were significantly decreased ( $P < 0.05$ ) in YAP<sup>deleted</sup> mice (Figure 2).

### YAP activation and deletion alters the alveolar epithelial cell populations *in vitro*

Alveolar organoids were produced from EPCAM+ cells isolated from YAP<sup>active</sup>, YAP<sup>deleted</sup>, and WT mice (cell population analyses available in Figure S1). EPCAM+ cells were isolated from mice of each genotype at PND14 and cultured for 21 days. Immunofluorescence analysis of SFTPC, AGER, and HOPX demonstrated that organoids produced from YAP<sup>active</sup> EPCAM+ cells had increased numbers of AT1 cells, whereas a mixture of AT2 (SFTPC+) and AT1 (AGER + HOPX+) cells were produced from WT mice (Figure 3A). Organoid forming efficiency and size were assessed. YAP<sup>active</sup> AT2 cells generated

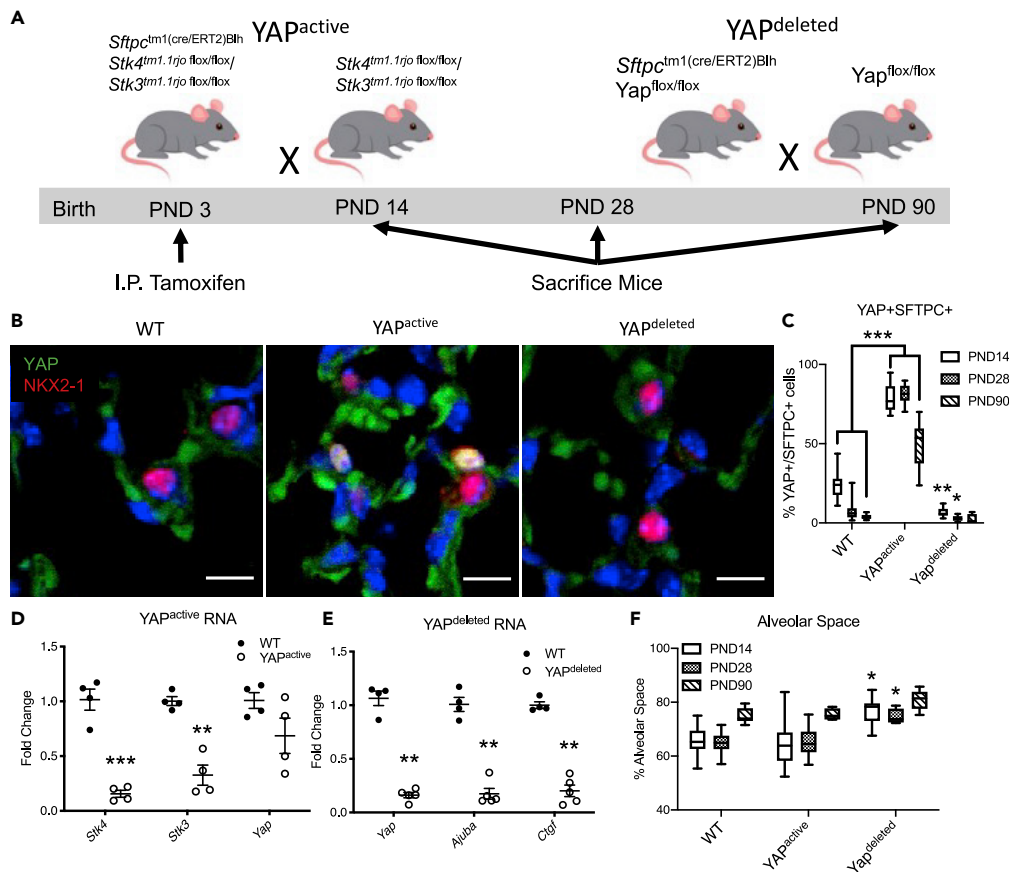


**Figure 1. YAP activation and deletion in mouse AT2 cells**

(A) Strategy and timeline of inducible deletion or activation of YAP. Mice were sacrificed at postnatal day (PND) 14, 28 and 90 for analysis.

(B) Immunofluorescence analysis of YAP (green) and NKX2-1 (red) and quantification of SFTPC+ AT2 cells with YAP+ nuclei at PND 14, 28, and 90 demonstrating increased nuclear YAP in YAP<sup>active</sup> mouse lungs.

(D and E) qRT-PCR analysis of YAP-related genes in isolated EPCAM+ cells following YAP activation (D) or deletion (E).

(F) Quantification of alveolar space in WT, YAP<sup>active</sup> and YAP<sup>deleted</sup> mouse lungs at PND 14, 28, and 90 demonstrating YAP<sup>deleted</sup> mouse lungs have increased alveolar space. \* Indicates p < 0.05 as determined by two-way ANOVA followed by Sidak's multiple comparison test. Dot plot graph error bars represent S.E.M and whiskers of Box-Whisker plots represent min and max values. \*\*p<0.001, \*\*\*p<0.0001.

more organoids that were smaller than those produced from WT mice (Figures 3B and 3C). EPCAM+ cells isolated from YAP<sup>deleted</sup> mice produced fewer organoids than those from WT cells. YAP<sup>deleted</sup> EPCAM+ cells produced organoids that were enriched for SFTPC+ cells and lacked HOPX+ AT1 cells (Figure 3D).

### Prediction of an alveolar epithelial cell transcriptional regulatory network

To further identify factors controlling AT1 and AT2 cell differentiation, we interrogated single-cell RNA sequencing data from E18.5 fetal mouse lung, a time of active AT1 and AT2 cell differentiation, to identify genes selectively expressed in AT1 and AT2 cells (Guo et al., 2019). We identified 401 AT1 associated genes and 403 AT2 associated genes (p < 0.05 and fold change > 1.5). Cell specific Transcription Regulatory Networks (TRN) were constructed using RNAs selectively expressed as potential targets and transcription factors expressed as potential regulators in AT1 or AT2 cells (Figure S2). The importance of a given transcription factor in the TRN was determined by measuring the combination of centrality and disruption using SINCERA (Guo et al., 2015). Transcription factors predicted to control AT2 cell differentiation included *Etv5*, *Sox9*, *Rbpj1* and *Tfcp2l1*. Transcription factors including *Nkx2-1* and chromatin modulators *Nfia*

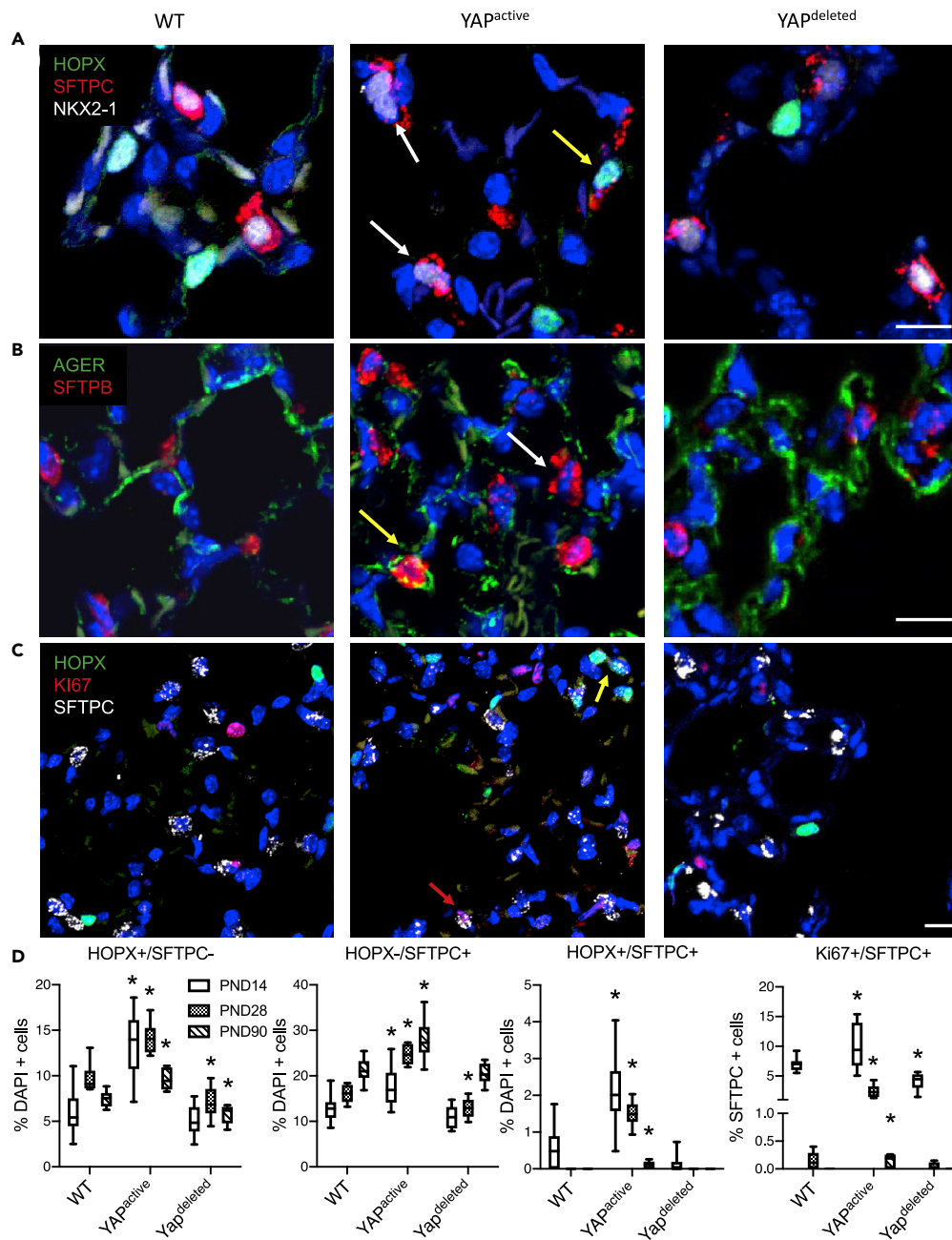


**Figure 2. YAP regulates alveolar epithelial cell differentiation**

(A–C) Immunofluorescence analysis of proliferation (Ki67), AT1 (HOPX, AGER), AT2 (SFTPC, SFTPB), and epithelial (NKX2.1) cell markers to assess alveolar epithelial cell proliferation and differentiation in YAP<sup>active</sup> and YAP<sup>deleted</sup> mouse lungs.

(D) Quantification of HOPX+/SFTPC- AT1, HOPX-/SFTPC+ AT2, HOPX+/SFTPC+ “dual positive” (yellow arrow) and Ki67+/SFTPC+ proliferating AT2 cells (red arrows) in PND14 (N = 11 WT, 12 YAP<sup>active</sup>, 10 YAP<sup>deleted</sup>), 28 (N = 9 WT, 9 YAP<sup>active</sup>, 8 YAP<sup>deleted</sup>), and 90 (N = 8 WT, 8 YAP<sup>active</sup>, 8 YAP<sup>deleted</sup>). SFTPC+ “doublets” are indicated with white arrows. Whiskers of box-whisker plots represent min and max values. \*Indicates p<0.05 as determined by Two-way ANOVA followed by Sidak’s multiple comparisons test.

and *Nfib*, were predicted as key regulators in both AT1 and AT2 cells. *Hopx*, *Elf3a*, *Klf5* and the YAP cofactor, *Tead1*, were predicted to regulate AT1 cell differentiation (Figure 4). The presence of *Tead1* in the AT1 TRN supported the concept that YAP, via TEAD activity, may interact in a transcriptional network regulating AT1 cell gene expression and differentiation.

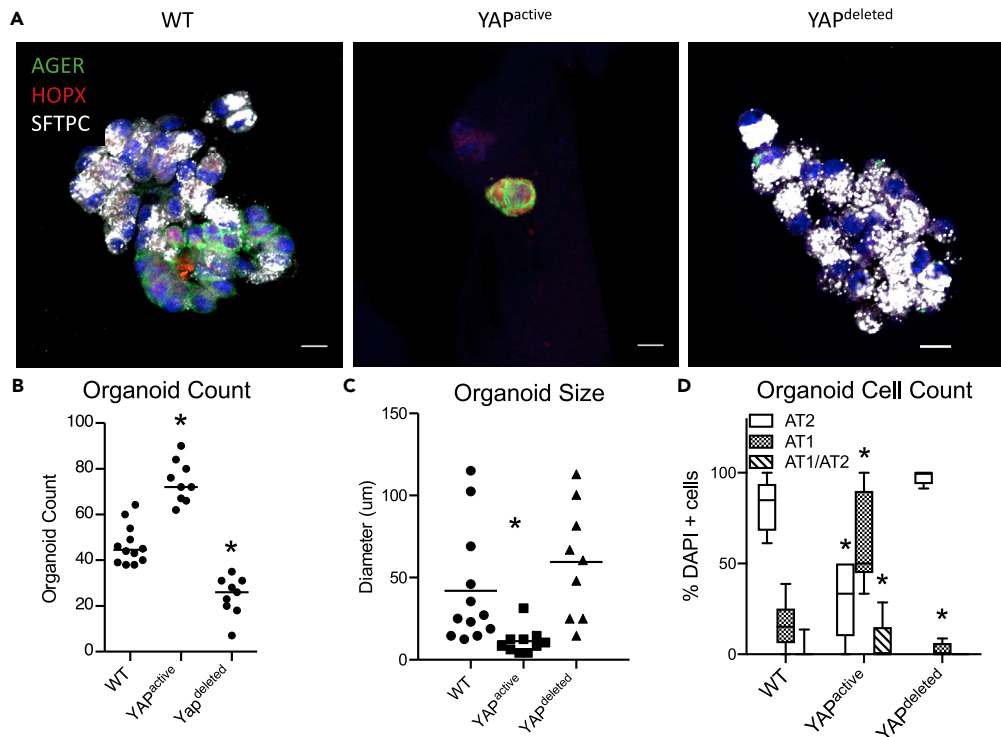


### Figure 3. YAP regulates growth and differentiation of alveolar organoids

(A) Immunofluorescence analysis of AGER (green), HOPX (red), and SFTPC (white) of organoids generated with WT control, YAP<sup>active</sup>, or YAP<sup>deleted</sup> EPCAM<sup>+</sup> cells.

(B) Quantification of organoids generated per well shows YAP<sup>active</sup> cells (N = 9) generate more organoids, while YAP<sup>deleted</sup> cells (N = 9) produced fewer than WT cells (N = 11).

(C) Analysis of average organoid size per well demonstrates YAP<sup>active</sup> cells generated smaller organoids than those produced with YAP<sup>deleted</sup> or WT EPCAM<sup>+</sup> cells.

(D) Quantification of cell-type specific markers demonstrate a shift in alveolar epithelial cell differentiation with more AT1 cells present in YAP<sup>active</sup> and less AT1 cells in YAP<sup>deleted</sup> organoids. Whiskers of box-whisker plots represent min and max values. See also Figure S1 for AEC purity during cell preparation. \*Indicates p<0.05 as determined by Two-way ANOVA followed by Sidak's multiple comparisons test.

### YAP deletion enhances expression of mature AT2 cell markers

To assess the role of YAP in the regulation of AT2 cell proliferation and AT1/AT2 cell differentiation, RNA and Assay for Transposase Accessible Chromatin (ATAC) sequencing were performed using EPCAM<sup>+</sup> cells isolated from YAP<sup>active</sup>, WT, and YAP<sup>deleted</sup> mouse lungs at PND14. ATAC-seq of isolated EPCAM<sup>+</sup> cells demonstrated that deletion of YAP had little effect on chromatin accessibility (Figure S3A), consistent with the paucity of *Yap* expression in normal mature alveolar epithelial cells. RNAs selectively expressed in mature AT2 cells, including *Abca3*, *Sftpb*, and *Napsa*, were increased in YAP<sup>deleted</sup> mice (Figure 5A). Deletion of YAP increased expression of genes involved in bioprocesses associated with mature AT2 cells, including "phospholipid biosynthetic process", "surfactant homeostasis", and "lipid metabolism" (Figure 5B). Consistent with deletion of *Yap*, expression of YAP target genes, including *Axl*, *Ajuba*, *Tead1*, and *Tead4* was reduced. Genes involved in bioprocesses including "regulation of cell migration", "positive regulation of cell population proliferation", and "epithelial cell differentiation", were suppressed consistent with reduction of YAP activity (Figure 5C). Since YAP<sup>deleted</sup> cells expressed high levels of AT2 cell signature genes and SOX9 was predicted to regulate AT2 cell differentiation (Figure 4), lung tissues were stained for SOX9. While all AT1 and AT2 cells identified in WT mice were SOX9 negative, a readily detectable, abnormal population of SOX9<sup>+</sup> SFTPC<sup>+</sup> "AT2 like" cells was observed in YAP<sup>deleted</sup> mice (Figure 5D).

### YAP activation increases expression of AT1 and proximal epithelial cell markers in AECs

Expression of genes associated with epithelial cell proliferation, including *Ccnd1* and *Cndk1*, were increased in EPCAM<sup>+</sup> cells isolated from YAP<sup>active</sup> mice. *Ager* and *Aqp5*, genes associated with AT1 cell

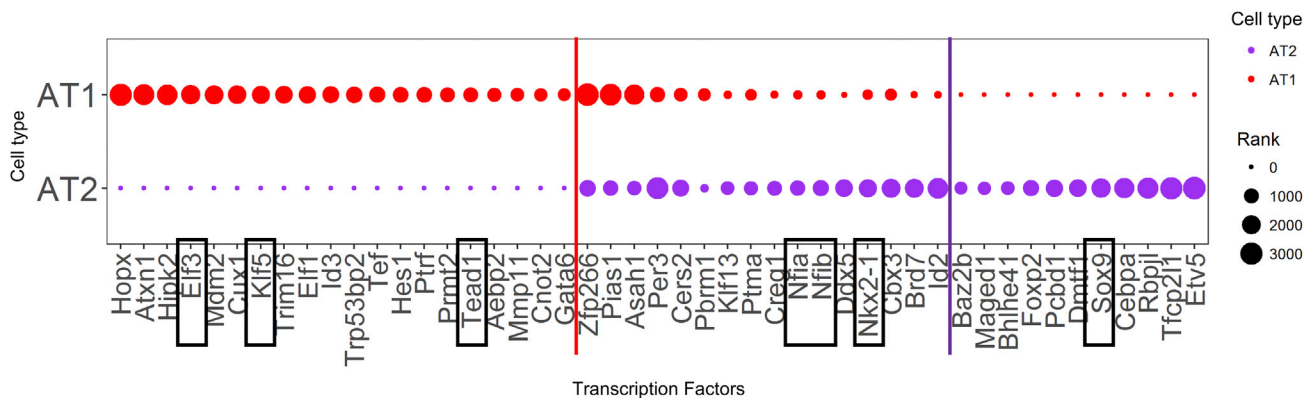


**Figure 4. Predicted alveolar epithelial cell transcriptional network**

Prediction of alveolar epithelial cell transcriptional regulatory network (TRN) from previously published single cell RNA sequencing data. AT1 or AT2 specific differentially expressed genes were used as potential target genes and transcriptional factors commonly or selectively expressed in AT1 or AT2 were identified as potential transcription factor regulators. Transcription factors were ranked based on their nodes importance to the inferred AT1 or AT2 TRNs using a method combining the six node importance metrics as described in SINCERA, with a higher rank score corresponding to a transcription factor being more important to a given TRN. The transcription factors *Elf3*, *Klf5* and *Tead1* were predicted as AT1 selective, and *Sox9* and *Etv5* were AT2 selective. *Nkx2-1*, *Nfia* and *Nfib* were predicted as important in both AT1 and AT2 cells. See also [Figure S2](#) for network information.

differentiation, were increased ([Figures 6A and 6D](#)), consistent with an increased number of AT1 and AT1/AT2 cells in YAP<sup>active</sup> mice. Genes induced in YAP<sup>active</sup> cells were associated with “epithelial cell differentiation”, “mitotic cell cycle”, “epithelial hyperplasia”, and “epithelial development” ([Figure 6B](#)). Within genes involved in “epithelial development”, genes associated with “idiopathic pulmonary fibrosis” and “abnormal type 1 pneumocyte morphology” were increased in YAP<sup>active</sup> EPCAM+ cells ([Figure 6C](#)). Genes associated with “mesenchymal development” and “extracellular matrix” were decreased in YAP<sup>active</sup> cells ([Table S1](#)). Predicted AT1 regulators *Klf5* and *Elf3* RNAs were induced in YAP<sup>active</sup> EPCAM+ cells as determined by qRT-PCR and RNAseq ([Figures 6A and 6D](#)). Immunofluorescence staining demonstrated that KLF5 was expressed in the “AT2 cell doublets” present in YAP<sup>active</sup> mice and in normal AT2 cells ([Figure 6E](#)). Expression of genes associated with IPF, including proximal epithelial cell markers *Muc5b*, *Scgb1a1*, *Scgb3a1*, and *Scgb3a2* were increased in YAP<sup>active</sup> EPCAM+ cells by RNA-seq and qRT-PCR ([Figures 6A and 6F](#)). Immunofluorescence staining of SCGB1A1, MUC5B, and SFTPC identified SCGB1A1+/SFTPC+ cells in YAP<sup>active</sup> mice, while none were detected in control mice with the antibodies used ([Figures 6G and S4](#)) consistent with abnormal epithelial cell differentiation. Analysis of MUC5B protein expression did not demonstrate co-expression in SFTPC+ AT2 cells ([Figure S4](#)), however, RNAScope analysis of *Muc5b* RNA expression showed the presence of *Sftpc*+/*Muc5b*+ cells in YAP<sup>active</sup> mice ([Figure 6H](#)). *Sftpc*+/*Scgb1a1*+ cells were identified by RNAScope, perhaps representing BASCs cells, in both WT and YAP<sup>active</sup> mice. Motif enrichment analyses of the promoters of genes induced by YAP were enriched for binding sites for transcription factors *Klf5*, *Elf3*, *Nr2f6*, and *Mycn* and these transcription factors were increased in YAP<sup>active</sup> epithelial cells ([Figure 6I](#)).

### Active YAP expression induces widespread increased accessibility of chromatin regions

Since YAP influenced expression of many genes involved in pulmonary epithelial cell differentiation, we tested YAP altered chromatin accessibility in EPCAM+ cells using ATAC-seq. YAP<sup>active</sup> epithelial cells had increased chromatin accessibility at more than 8400 genomic regions, of which 3864 were located in regions defined as gene promoters. Several genomic regions were less accessible in YAP<sup>active</sup> mice, of which only 70 were in gene promoter regions ([Figure 7A and S3B](#)). Functional enrichment analyses of promoters opened in YAP<sup>active</sup> epithelial cells were mapped to genes associated with “cell cycle”, “proliferative AT2 progenitor”, “AT1 cell precursor”, and “PND3 epithelial subtype AT1” ([Figure 7B](#)). Motif enrichment analyses of chromatin regions opened in YAP<sup>active</sup> mice were enriched for binding sites for transcription factors KLF5, NKX2.1, ELF3 and NF1, and coincided with increased expression of *Klf5* and *Elf3* RNAs ([Figure 7C](#)). KLF5 and NFIB binding sites were identified in promoter regions of genes with YAP induced chromatin accessibility. Promoter regions of the *Klf5* and *Nfib* genes were also opened ([Figure 7D](#)). Since the promoters of genes with altered expression in YAP<sup>active</sup> epithelial cells were enriched for NFIB binding sites, immunofluorescence analysis was used to test whether NFIB was expressed in AT2 cells.

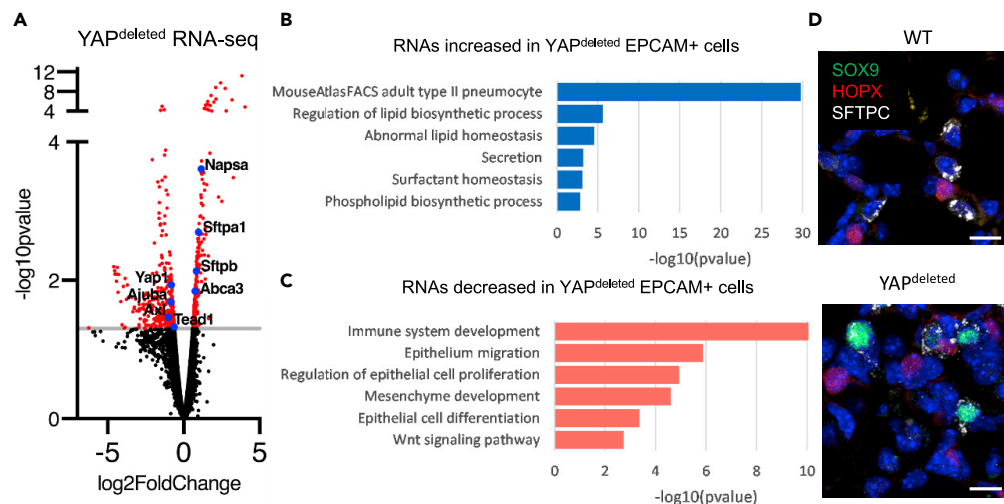


### Figure 5. YAP deletion increases expression of AT2 cell signature genes

RNA-seq analyses were performed on EPCAM<sup>+</sup> cells isolated from PND14 YAP<sup>deleted</sup> (N = 5) and WT (N = 4) mice. (A) Volcano plot of the differentially expressed genes ( $p < .05$ , FC > 1.5) shows increase in AT2 markers *Abca3*, *Sftpb* and *Sftpa1*, and decrease in known YAP targets *Ajuba*, *Axl* and *Yap* itself. (B) Functional enrichment analyses of the induced genes associated with *lipid* and *surfactant* production. (C) Functional enrichment analyses of the suppressed genes show decreased gene expression associated with *Wnt* signaling, *Immune* and *Mesenchyme* development, *Epithelial cell migration* and *proliferation* and *Epithelial cell differentiation*. (D) Immunofluorescence analysis of SOX9 (green) and SFTPC (white) demonstrates the presence of SOX9<sup>+</sup>/SFTPC<sup>+</sup> epithelial cells in YAP<sup>deleted</sup> mice. See Figure S3 for further ATAC-seq quality control.

Nuclear NFIB was detected in a subset of SFTPC<sup>+</sup> cells in both YAP<sup>active</sup> and WT mice (Figure 7E). Together, these data demonstrate that YAP regulates chromatin accessibility in putative *Klf5* and *Nfib* regulatory regions, both being factors predicted to influence AT2/AT1 cell differentiation.

### YAP and NFIB directly interact

NFI family members influence chromatin remodeling (Denny et al., 2016); thus, we hypothesized that NFIB may interact with the HIPPO/YAP pathway to open chromatin and influence alveolar epithelial cell gene expression. We co-expressed constitutively active, flag-tagged YAP(S127A) and HA-tagged NFIB in human bronchial epithelial (HBEC3) cells. Co-immunoprecipitation assays of Flag-YAP(S127A) and HA-NFIB demonstrated that these proteins co-immunoprecipitated (Figures 8A and S6). We were unable to demonstrate that YAP directly interacts with NKX2-1 or KLF5 using available antibodies in HBEC3s; however, direct interactions between YAP and KLF5 (Zhi et al., 2012) and NKX2-1 (Otsubo et al., 2017) were previously shown in MCF10A breast cancer cells and C22 mouse airway progenitor cells, respectively.

### YAP, NKX2-1, and NFIB induce KLF5 promoter activity

Since NFIB binding sites were identified in the promoter regions of the *Klf5* gene that were opened in YAP<sup>active</sup> mice, and *Klf5* RNA was increased in YAP<sup>active</sup> mice, we sought to identify whether YAP or NFIB regulated *Klf5* promoter activity. A *KLF5* luciferase construct containing 2kb of the *KLF5* promoter region was used. Multiple TEAD binding sites were identified within this 2kb promoter region, along with predicted NKX2-1 and NFIB binding sites (Figure S5A and S5B). While NFIB and NKX2-1 expression was not sufficient to induce *KLF5*-luciferase activity, co-expression of NFIB, NKX2-1, and constitutively active (S127A)YAP markedly increased *KLF5*-luciferase activity demonstrating that YAP interacts with NKX2-1 and NFIB to regulate the *KLF5* promoter *in vitro* (Figure 8B). Consistent with this finding, meta-analysis of publicly available YAP1 CHIP-seq data demonstrated that YAP binds to the *KLF5* promoter at a site 3kb upstream of the *KLF5* transcriptional start site in NCI H2052 and MDA MB 231 cells (Stein et al., 2015) (Figure S5B).

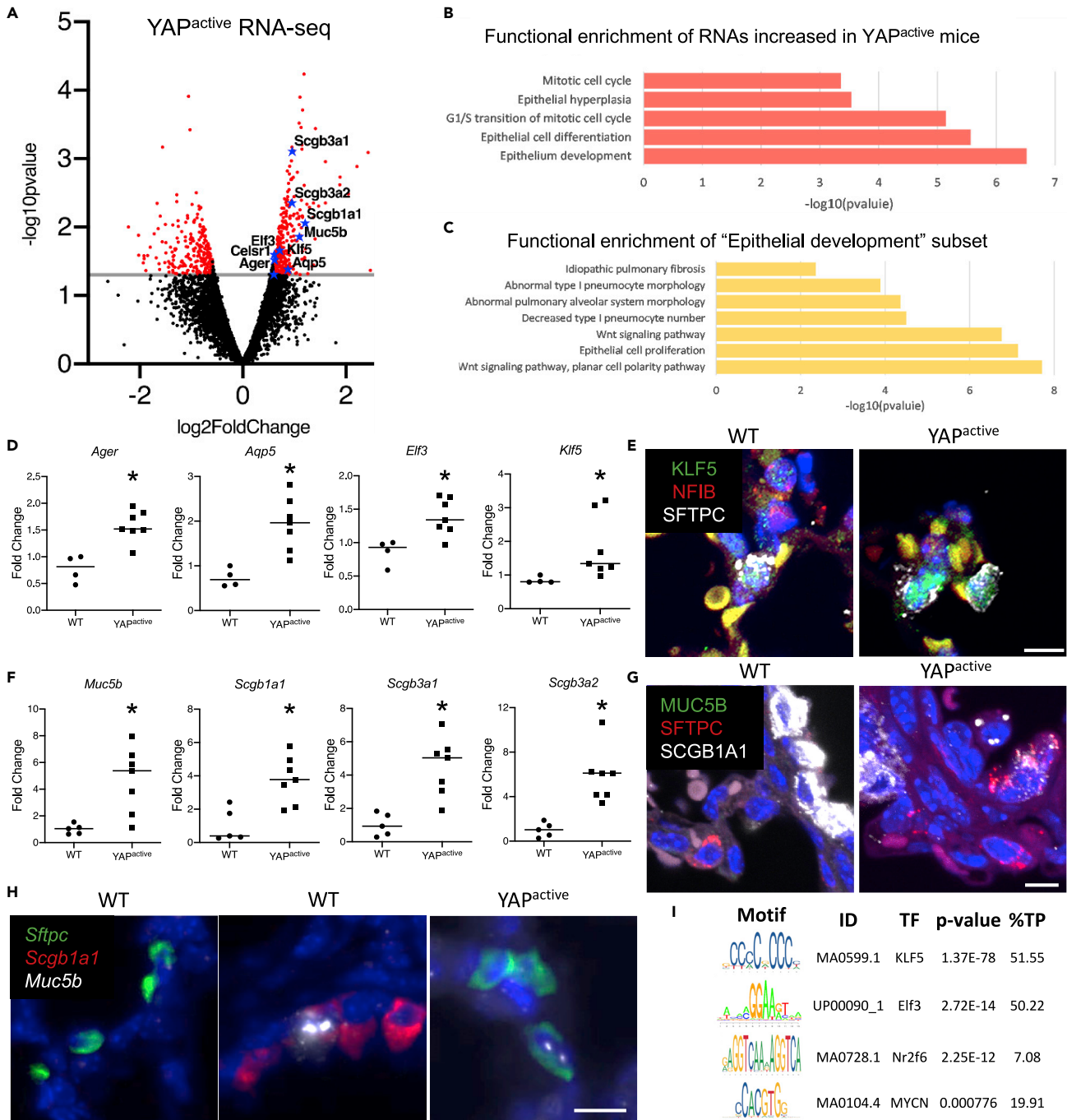


**Figure 6. YAP activation increases expression of AT1 and proximal epithelial cell signature genes**

RNA-seq analyses were performed on EPCAM<sup>+</sup> cells isolated from D14 YAP<sup>active</sup> (N = 6) and controls (N = 4) mice.

(A) Volcano plot of the differentially expressed genes ( $p < .05$ , FC > 1.5) shows increase in AT1 markers *Ager* and *Aqp5* as well as proximal lung airway markers *Muc5b*, *Scgb1a1*, *Scgb3a1* and *Scgb3a2*.

(B) Genes upregulated in the YAP<sup>active</sup> epithelium are associated with mitotic cell cycle and epithelial cell differentiation and development.

(C) Functional enrichment analyses of the subset of genes associated with epithelium development revealed increases in the expression of genes associated with Wnt signaling, epithelium proliferation, IPF and abnormal AT1 differentiation.

(D) Realtime qRT-PCR analyses of isolated YAP<sup>active</sup> epithelial cells demonstrate increased *Ager*, *Aqp5*, *Elf3* and *Klf5*. \*Indicates  $p < 0.05$  as determined by Welch's *t*-test.

**Figure 6. Continued**

- (E) Immunofluorescence analysis of NFIB (red), KLF5 (green), and SFTPC (white) shows presence of KLF5 in SFTPC+ cells including the SFTPC+ AT2 cell doublets identified in YAP<sup>active</sup> mice.
- (F) qRT-PCR analysis of proximal cell signature genes demonstrate increased conducting airway epithelial cell markers in YAP<sup>active</sup> epithelial cells. \*Indicates  $p < 0.05$  as determined by Welch's t-test.
- (G) Immunofluorescence analysis of MUC5B (green), SFTPC (red), and SCGB1A1 (white), shows the presence of SCGB1A1+/SFTPC+ cells in YAP<sup>active</sup> mice.
- (H) RNAscope Fluorescent *in-situ* hybridization of *Muc5b*, *Scgb1a1*, and *Sftpc* in WT and YAP<sup>active</sup> mouse lungs demonstrating the presence of *Sftpc*+/*Muc5b*+ cells in YAP<sup>active</sup> lungs.
- (I) Promoter analyses of the genes increased in the YAP<sup>active</sup> epithelium show that transcription factors *Klf5*, *Elf3*, *Nr2f6*, and *Mycn* RNAs are increased and have enriched binding sites in YAP<sup>active</sup> induced genes. See [Table S1](#) for pathways down regulated in YAP<sup>active</sup> mice and [Figure S4](#) for immunofluorescence images.

**YAP, TEAD, NKX2-1, and NFIB interact to increase expression and promoter activity of the AT1 cell marker AGER**

Since present findings supported a role for YAP and KLF5 in promoting AT1 cell-associated gene expression, we tested their effect on the expression of *AGER*, a known AT1 cell signature gene. Conserved KLF5, NFIB, NKX2-1, and TEAD binding sites were identified in the *AGER* promoter region located approximately 1.5kb from the transcriptional start site ([Figure S5C](#)). Co-expression of (S127A)YAP and KLF5 enhanced human *AGER* promoter luciferase activity ([Figure 8C](#)) and co-transfection of (S127A)YAP with KLF5 and/or NKX2-1 synergistically increased *AGER* RNA in HBEC3 cells, a cell line that normally does not express *AGER* ([Figure 8D](#)). To assess whether responses to YAP were mediated by TEAD, TEADs 1-4 were inhibited with siRNA in HBEC3 cells co-transfected with YAP, KLF5, and NKX2-1. The inhibition of TEADs reduced expression of *AGER* RNA ([Figure 8E](#)). To determine the role of the TEAD, NFIB, and NKX2-1 binding sites within the *AGER* promoter, site-directed mutagenesis was used to alter the binding sites of each transcription factor ([Figure 8F](#)). Mutagenesis of either NKX2-1, TEAD, or NFIB binding sites within the *AGER* promoter inhibited the YAP/NKX2-1/KLF5 induced *AGER* luciferase activity ([Figures 8G](#) and [S5C](#)). Taken together these data support a model in which YAP regulates chromatin remodeling and transcriptional activation in alveolar progenitor cells. YAP, in concert with NFIB, influences chromatin accessibility in promoter regions of genes regulating alveolar epithelial cell differentiation. YAP, KLF5, NFIB, and NKX2-1 interacted to activate the AT1 signature gene *AGER*, a process, at least in part, regulated by TEADs ([Figure 8H](#)). Taken together, YAP participates in a transcriptional and chromatin mediated regulatory network with KLF5, NFIB, and NKX2-1 to influence pulmonary epithelial cell proliferation and differentiation.

**DISCUSSION****YAP/TEAD interact with a complex of transcription factors**

We used single cell RNA-seq data ([Guo et al., 2019](#)) to construct a gene regulatory network to predict the nodal importance of transcription factors regulating AT1 cell associated gene expression during late gestation, a time of alveolar epithelial cell proliferation and differentiation. KLF5, NFIB, NKX2-1, and TEAD1, the latter a mediator of YAP transcriptional activity, were strongly associated with AT1 gene expression. These findings are consistent with previous studies demonstrating critical roles for KLF5 ([Wan et al., 2008](#)), NFIB ([Hsu et al., 2011](#)), and NKX2-1 ([Little et al., 2019](#); [Wert et al., 2002](#)) in alveolar formation, maturation, and differentiation. Together with YAP, these transcription factors and their target genes play critical roles in alveolar formation and repair. Present ATAC-seq data and gene expression studies further support the role of a YAP mediated regulatory network, wherein YAP promotes widespread chromatin changes in promoter regions of key transcription factors and predicted targets. Likewise, *in vitro* studies demonstrated that YAP was required for the coordinated transcriptional activities of NFIB, KLF5, and NKX2-1 to induce the AT1 signature gene *AGER* partially in a TEAD dependent manner. The transcription factor NKX2-1 plays a major role in regulating respiratory epithelial cell fate decisions. Recent findings demonstrate that NKX2-1 is present in AT1 cells, and deletion of NKX2-1 in AT2 cells leads to loss of respiratory epithelial cell identity, resembling gastrointestinal cells ([Little et al., 2019](#)). During the process of revising this work, a recent publication demonstrated findings consistent with the present work showing that NKX2-1 plays different roles in AT1 and AT2 cells, and that as AT1 or AT2 cells "mature", NKX2-1 interacting partners change and this is in part regulated by YAP in AT1 cells ([Little et al., 2021](#)). The potential role of YAP/NKX2-1 interaction is unclear, however, in C22 mouse airway progenitor cells, YAP and NKX2-1 directly interact to negatively regulate the NKX2-1 target *Col17a1* ([Otsubo et al., 2017](#)). Likewise, NKX2-1 directly binds NFIB in cultured lung epithelial cells ([Hsu et al., 2011](#)). Deletion of NFIB in the mouse lung results in alveolar simplification with loss of AT2 and AT1 cell differentiation ([Hsu et al., 2011](#)). YAP directly

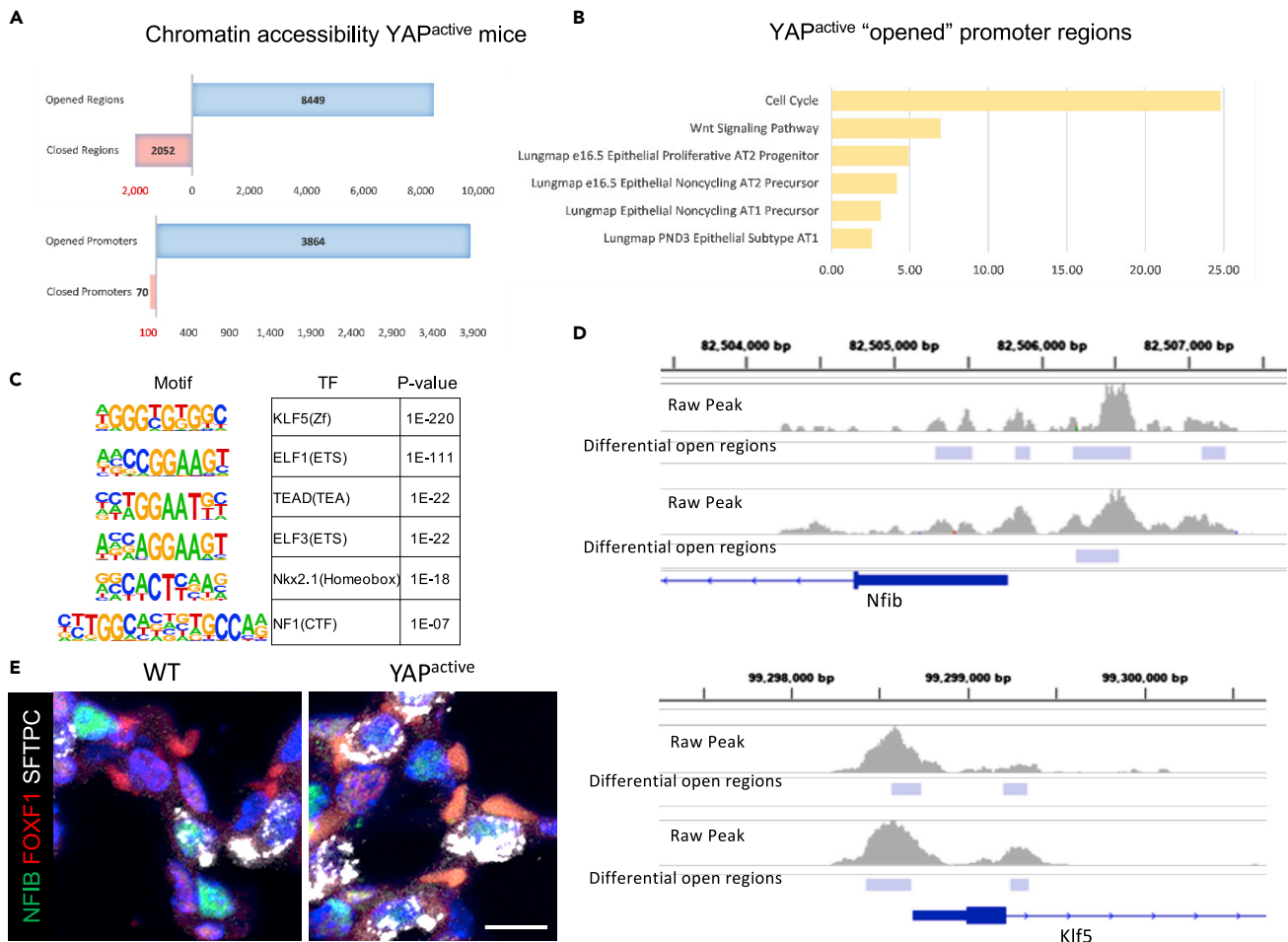


**Figure 7. YAP regulates chromatin accessibility of promoter regions in genes associated with alveolar differentiation**

ATAC-seq was performed on EPCAM<sup>+</sup> cells isolated from PND14 YAP<sup>active</sup> (N = 3) and WT (N = 3) mice.

(A) YAP activation opened over 8400 regions of DNA and closed 2052 regions ( $p < .01$ ). Over 3800 gene promoters (1.5kb of predicted transcriptional start site) were opened in YAP<sup>active</sup> epithelial cells with only 70 promoters being closed.

(B) Functional enrichment analyses of genes with opened promoters opened in YAP<sup>active</sup> mice show increased accessibility of signature genes for various AT1 and AT2 subtypes along with genes involved in *Wnt signaling* and *cell cycle*.

(C) Motif enrichment analyses of the regions opened in YAP<sup>active</sup> mice show an enrichment for multiple transcription factors that were predicted regulators of the AT1 and/or AT2 cell TRN.

(D) IGV was used to visualize regions opened in *Nfib* and *Klf5* promoter regions in YAP<sup>active</sup> epithelial cells. ATAC-seq analyses were done using Mac2 on 2 litters, with YAP<sup>active</sup> (N = 3) compared to *Stk3<sup>fllox/fllox</sup>Stk4<sup>fllox/fllox</sup>* (N = 3) control littermates. Only regions altered in both litters were considered significant.

(E) Immunofluorescence analysis of NFIB (green), FOXF1 (red), and SFTPC (white) demonstrates NFIB in a subset of SFTPC<sup>+</sup> cells in both WT and YAP<sup>active</sup> mouse lungs. See [Figure S3](#) for analysis of ATAC-seq quality.

interacts with NFIB to regulate cancer cell proliferation (Pajtler et al., 2019); likewise, YAP and KLF5 directly interact to regulate cardiac progenitor cell proliferation and differentiation (Zhi et al., 2012). In the lung, deletion of KLF5 impairs perinatal lung sacculation and AT1 cell differentiation (Wan et al., 2008). KLF5 regulates epithelial cell differentiation in other organs including the gut (Bell et al., 2011, Bell et al., 2013). KLF5 regulates epithelial cell proliferation in several cancers and cancer cell lines, including A549 cells, and YAP/KLF5 interactions promote breast cancer proliferation (Zhi et al., 2012; Zhao et al., 2018). Collectively these findings strongly suggest that YAP, TEAD, KLF5, NFIB, and NKX2-1 participate in a gene network regulating lung epithelial proliferation and differentiation.

### YAP/TEAD directly regulate AT1 cell differentiation

We have demonstrated that YAP regulates the promoter activity and transcription of the AT1 marker gene *AGER*, in a TEAD-dependent manner that is blocked by altering TEAD binding sites within the *AGER*

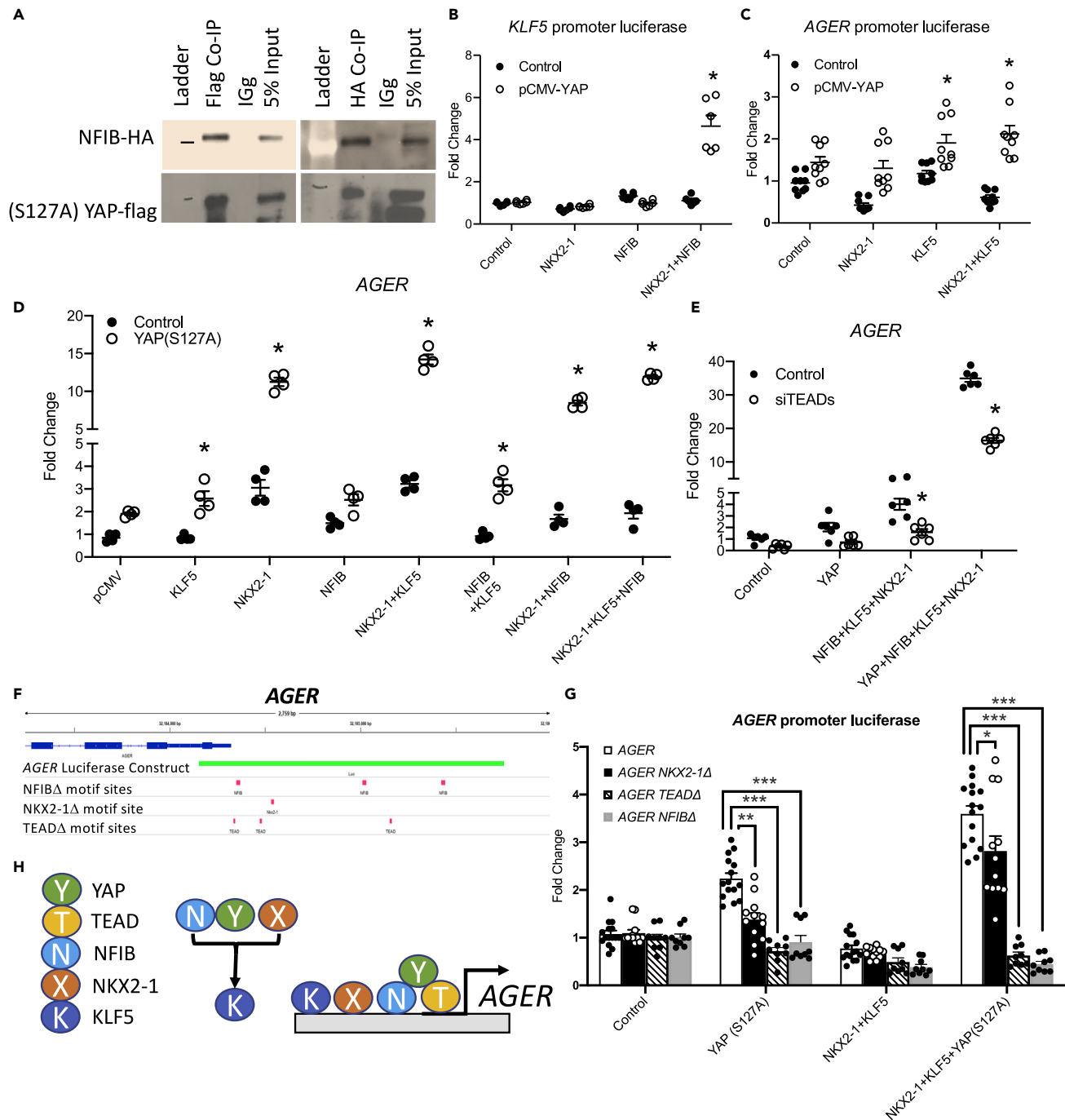


**Figure 8. YAP interacts with NFIB, KLF5, and NKX2-1 to regulate gene expression**

(A) Immunoprecipitation assay of HBEC3 cells co-expressing (S127A)YAP-FLAG and GFP-NFIB-HA constructs demonstrating YAP and NFIB co-precipitate. (B) HBEC3 cells co-expressing (S127A)YAP, KLF5, and NKX2-1 activate *KLF5* promoter luciferase activity. (C) HBEC3 cells co-transfected with (S127A)YAP, NKX2-1, and KLF5 activate *AGER* promoter luciferase. (D) HBEC3 cells co-expressing empty pCMV vector, KLF5, NKX2-1, NFIB, and (S127A)YAP increase *AGER* RNA assessed by qRT-PCR. (E) *AGER* RNA was measured in HBEC3 cells co-transfected with pCMV empty vector (control), (S127A)YAP, NFIB, KLF5, and NKX2-1 with siRNAs targeting TEADs 1-4. *AGER* induction is partially inhibited by TEAD siRNAs. Graphs are representative of multiple (N > 3) experiments. (F) A schematic of the *AGER* promoter and luciferase assay with locations of predicted TEAD, NKX2-1, and NFIB binding sites that were mutated to assess DNA binding of respective transcription factors to the *AGER* promoter.

**Figure 8. Continued**

(G) HBEC3 cells expressing NKX2-1, KLF5, and YAP in the presence of *AGER* luciferase constructs with five site mutations in predicted binding sites of TEAD (TEAD $\Delta$ ), NKX2-1 (NKX2-1 $\Delta$ ) or NFIB (NFIB $\Delta$ ). Altering the predicted binding sites of NKX2-1 ( $p < 0.05$ ), TEAD ( $p < 0.0001$ ), or NFIB ( $p < 0.0001$ ) significantly reduced *AGER* promoter activation by YAP, KLF5, and NKX2-1.

(H) A schematic of NFIB, KLF5, NKX2-1, YAP, and TEAD interacting on the *AGER* promoter to induce *AGER* transcription. See Figure S5 for further information and Figure S6 for full size co-immunoprecipitation blots. \*Indicates  $p < 0.05$  as determined by Two-way ANOVA followed by Sidak's multiple comparisons test. \*\* $p < 0.001$ , \*\*\* $p < 0.0001$ .

promoter. We show that postnatal activation of YAP via deletion on *Stk3/Stk4* is sufficient to increase AT1 cell differentiation. Present findings are consistent with previous reports demonstrating increased expression of AT1 signature genes in cultured airway epithelial cells (Lange et al., 2015), and previous reports that activation of YAP, via deletion of *LATS1/2* at E17.5 or expression of YAP(S127A) at E15.5, increases numbers of AT1 cells at birth (Nantie et al., 2018). Recent lineage tracing studies and single cell analyses of the embryonic mouse lung demonstrated that during normal development, AT1 cell specification is completed by E17.5 (Frank et al., 2019). During revision, a recent manuscript has demonstrated that YAP knockout in AT1 cells leads to an "exaggerated" AT2 cell phenotype and activation of YAP leads to the presence of cells expressing AT1 and AT2 cell markers consistent with our findings (Penkala et al., 2021). Herein, we demonstrate that activation of YAP in the postnatal lung enhances AT1 cell numbers, indicating that AT1/AT2 specification and differentiation by bipotent progenitors can be activated after birth without injury in the perinatal lung.

**YAP regulates progenitor cell fate decisions**

We demonstrated that YAP enhanced proliferation and influenced differentiation of alveolar progenitor cells in the postnatal lung. Embryonic activation or deletion of YAP was lethal in transgenic mouse models (Dai et al., 2017; Lange et al., 2015; Mahoney et al., 2014; van Soldt and Cardoso, 2020). Deletion of the YAP homologue TAZ during embryonic development caused alveolar simplification and an emphysema-like phenotype, while deletion of YAP/TAZ impaired AT2 cell proliferation and AT1 cell differentiation (Lacanna et al., 2019; Mitani et al., 2009). Activation of nuclear YAP in cultured human airway cells and genetic models of YAP activation in mouse airway cells caused terminal differentiation and loss of basal progenitor cells (Lange et al., 2015; Mahoney et al., 2014; van Soldt et al., 2019). Nuclear YAP was dynamically regulated after naphthalene mediated depletion of airway club cells, with increased YAP observed during the proliferative phase of recovery followed by its rapid loss after epithelial differentiation and regeneration. YAP deletion during the proliferative phase of recovery caused failure of progenitor cell self-renewal (Lange et al., 2015), indicating the importance of the dynamic regulation of YAP during lung development and repair. Since recent studies demonstrated an important role for Wnt responsive Axin2+ alveolar progenitor cells in the repair of the alveoli following influenza infection (Frank et al., 2016; Zacharias et al., 2018), we assessed changes in chromatin accessibility in promoter regions of *Wnt7b* and *Celsr1*, genes mediating Wnt signaling (Wang et al., 2005). YAP enhanced transcription and opened chromatin in promoter regions of both genes, perhaps indicating crosstalk between YAP and Wnt signaling in alveolar epithelial progenitor cell differentiation (Piersma et al., 2015; Wang et al., 2014). YAP is known to regulate the  $\beta$ -catenin destruction complex and activate  $\beta$ -catenin in cancer cell lines (Deng et al., 2018; Azzolin et al., 2014). Conversely, *Wnt5a* and *Wnt3a* enhance YAP activity in cancer (Park et al., 2015). The mechanisms by which these developmental pathways intersect to regulate alveolar epithelial cell proliferation and cell fate decisions warrant further study.

**Active epithelial YAP signaling induces a transcriptional network associated with IPF**

The alveolar epithelium has a remarkable capacity to regenerate after acute injury, wherein subsets of AT2 cells self-renew and rapidly differentiate into mature AT2 and AT1 cells. Failures in normal repair processes contribute to pulmonary fibrosis and tissue remodeling associated with chronic interstitial lung disease including idiopathic pulmonary fibrosis (IPF), chronic obstructive pulmonary disease (COPD), and emphysema. Herein, we identify the Hippo/YAP pathway as an important regulator of alveolar epithelial cell proliferation and differentiation in the postnatal lung. Activation of YAP in *in vitro* organoids induced AT1 cell differentiation from isolated AT2 cells, while YAP deletion blocked AT1 cell and enhanced AT2 cell differentiation. Activation of YAP during the postnatal period of mouse lung development resulted in abnormal alveolar epithelial cell proliferation and "indeterminate" epithelial cell differentiation. Atypically differentiated cells co-express genes characteristic of AT1, AT2, and conducting airway epithelial cells, genes normally tightly restricted to distinct epithelial cell types, were identified in YAP<sup>active</sup> mice. Previous

findings demonstrate increased YAP activity and the presence of similar indeterminate, non-lineage restricted epithelial cells in lung tissues from patients with IPF, supporting a role for Hippo/YAP signaling in the pathogenic alveolar remodeling characteristic of interstitial lung diseases (Gokey et al., 2018; Xu et al., 2016). Activation of YAP *in-vivo* caused widespread chromatin accessibility changes in regulatory regions of transcription factors that regulate pulmonary epithelial cell gene expression. Functional enrichment analysis of YAP-mediated RNA expression and chromatin accessibility predicted a new role for YAP in a transcriptional network consisting of KLF5, NFIB, and NKX2-1 which interact to regulate alveolar epithelial cell differentiation.

### Limitations of the study

Defining whether YAP directly or indirectly interacts with KLF5 or NKX2-1 to regulate transcription will be necessary to further elucidate the role of these interactions in AT1 cell differentiation. While YAP directly interacted with KLF5 and TTF1 (Zhi et al., 2012; Otsubo et al., 2017), we were not able to show this using the antibodies and methods we tested. Future experiments testing genetic interactions or ChIP experiments could shed light on how these transcription factors interact with YAP to regulate alveolar epithelial progenitor cell differentiation. Understanding how YAP differentially regulates Wnt-responsive AEPs compared to other AT2 cell subpopulations reveals a limitation within our study. Careful lineage tracing studies following YAP activation or deletion during development or repair models would provide further insight into the role of YAP in specific subsets of AT2 cell populations. The specific role of YAP in AT2 cell subtypes could also be tested utilizing our organoid model. Since the AT2 cells are YAP<sup>active</sup> or YAP<sup>deleted</sup> at the onset of organoid culture, future experiments are needed to define temporal changes in cell states regulated by YAP. Future organoid culture models could also address a limitation of our *in-vitro* analysis to assess how YAP, KLF5, NFIB, TEAD, and NKX2-1 interact. While using a more “alveolar” cell type may provide more direct analysis of AT2/AT1 cell differentiation, readily transfectable human alveolar epithelial cell lines are not currently available. We utilized immortalized proximal airway epithelial HBEC3 cells, which provide a readily transfectable cell line to assess the *in-vitro* interactions of these transcription factors in activating the AT1 cell marker *AGER*.

### STAR★METHODS

Detailed methods are provided in the online version of this paper and include the following:

- KEY RESOURCES TABLE
- RESOURCE AVAILABILITY
  - Lead contact
  - Materials availability
  - Additional information
  - Data and code availability
- EXPERIMENTAL MODEL AND SUBJECT DETAILS
- METHOD DETAILS
  - Immunofluorescence analysis
  - RNAScope
  - Alveolar epithelial cell enrichment
  - Organoid culture
  - Cell culture and transfections
  - Co-immunoprecipitation
  - Gene promoter assays
  - RNA analysis
  - ATAC-seq analysis
  - Bioinformatics
  - Quantification and statistical analysis

### SUPPLEMENTAL INFORMATION

Supplemental information can be found online at <https://doi.org/10.1016/j.isci.2021.102967>.

### ACKNOWLEDGMENTS

The authors would like to thank Jaymi Semona for assistance in mouse colony maintenance. We would like to thank Julia Bazzano and Chase Taylor for assistance in FACS analysis of isolated cells. This work was

made possible by the Pulmonary Fibrosis Foundation, by an independent grant from Boehringer Ingelheim Pharmaceuticals, Inc. who provided the financial support. The authors meet criteria for authorship as recommended by the International Committee of Medical Journal Editors (ICMJE) and were fully responsible for all aspects of the trial and publication development. This work was funded by the Pulmonary Fibrosis Foundation Scholars program (JJG), NIH T32 HL007752-24 training grant (JAW, JJG), U01 HL148856 (JAW, YX), U01HL134745 (JAW) and R01HL136722(JAW).

## AUTHOR CONTRIBUTIONS

Conceptualization: JJG, JS, AS, JAW; Methodology: JJG, JS, AS; Validation: JJG, AS, JK; Formal Analysis: JJG, JS, AS, PS; Investigation: JJG, AS, JK; Data Curation: JS, PS; Writing Original Draft: JJG, JS, AS, JAW; Writing Review and Editing: JJG, JS, AS, YX, JAW; Visualization: JJG, JS, AS; Supervision: JJG, JAW.

## DECLARATION OF INTERESTS

The authors declare no competing interests.

Received: August 14, 2020

Revised: February 26, 2021

Accepted: August 6, 2021

Published: September 24, 2021

## REFERENCES

- Afgan, E., Baker, D., Batut, B., van den Beek, M., Bouvier, D., Cech, M., Chilton, J., Clements, D., Coraor, N., Gruning, B.A., et al. (2018). The Galaxy platform for accessible, reproducible and collaborative biomedical analyses: 2018 update. *Nucleic Acids Res.* 46, W537–W544.
- Azzolin, L., Panciera, T., Soligo, S., Enzo, E., Bicciato, S., Dupont, S., Bresolin, S., Frasson, C., Basso, G., Guzzardo, V., et al. (2014). YAP/TAZ incorporation in the beta-catenin destruction complex orchestrates the Wnt response. *Cell* 158, 157–170.
- Barkauskas, C.E., Cronce, M.J., Rackley, C.R., Bowie, E.J., Keene, D.R., Stripp, B.R., Randell, S.H., Noble, P.W., and Hogan, B.L. (2013). Type 2 alveolar cells are stem cells in adult lung. *J. Clin. Invest.* 123, 3025–3036.
- Barnett, D.W., Garrison, E.K., Quinlan, A.R., Stromberg, M.P., and Marth, G.T. (2011). BamTools: AC++ API and toolkit for analyzing and managing BAM files. *Bioinformatics* 27, 1691–1692.
- Bell, S.M., Zhang, L., Mendell, A., Xu, Y., Haitchi, H.M., Lessard, J.L., and Whitsett, J.A. (2011). Kruppel-like factor 5 is required for formation and differentiation of the bladder urothelium. *Dev. Biol.* 358, 79–90.
- Bell, S.M., Zhang, L., Xu, Y., Besnard, V., Wert, S.E., Shroyer, N., and Whitsett, J.A. (2013). Kruppel-like factor 5 controls villus formation and initiation of cytodifferentiation in the embryonic intestinal epithelium. *Dev. Biol.* 375, 128–139.
- Besnard, V., Matsuzaki, Y., Clark, J., Xu, Y., Wert, S.E., Ikegami, M., Stahlman, M.T., Weaver, T.E., Hunt, A.N., Postle, A.D., et al. (2010). Conditional deletion of Abca3 in alveolar type II cells alters surfactant homeostasis in newborn and adult mice. *Am. J. Physiol. Lung Cell Mol. Physiol.* 298, L646–L659.
- Besnard, V., Wert, S.E., Stahlman, M.T., Postle, A.D., Xu, Y., Ikegami, M., and Whitsett, J.A. (2009). Deletion of Scap in alveolar type II cells influences lung lipid homeostasis and identifies a compensatory role for pulmonary lipofibroblasts. *J. Biol. Chem.* 284, 4018–4030.
- Bridges, J.P., Sudha, P., Lipps, D., Wagner, A., Guo, M., DU, Y., Brown, K., Filuta, A., Kitzmiller, J., Stockman, C., et al. (2020). Glucocorticoid regulates mesenchymal cell differentiation required for perinatal lung morphogenesis and function. *Am. J. Physiol. Lung Cell Mol. Physiol.* 319, L239–L255.
- Bridges, J.P., Wert, S.E., Noguee, L.M., and Weaver, T.E. (2003). Expression of a human surfactant protein C mutation associated with interstitial lung disease disrupts lung development in transgenic mice. *J. Biol. Chem.* 278, 52739–52746.
- Buenrostro, J.D., Wu, B., Chang, H.Y., and Greenleaf, W.J. (2015). ATAC-seq: A method for assaying chromatin accessibility genome-wide. *Curr. Protoc. Mol. Biol.* 109, 21 29 1–9.
- Cardoso, W.V. (2001). Molecular regulation of lung development. *Annu. Rev. Physiol.* 63, 471–494.
- Chen, J., Bardes, E.E., Aronow, B.J., and Jegga, A.G. (2009). ToppGene Suite for gene list enrichment analysis and candidate gene prioritization. *Nucleic Acids Res.* 37, W305–W311.
- Corti, M., Brody, A.R., and Harrison, J.H. (1996). Isolation and primary culture of murine alveolar type II cells. *Am. J. Respir. Cell Mol. Biol.* 14, 309–315.
- Cutz, E., Wert, S.E., Noguee, L.M., and Moore, A.M. (2000). Deficiency of lamellar bodies in alveolar type II cells associated with fatal respiratory disease in a full-term infant. *Am. J. Respir. Crit. Care Med.* 161, 608–614.
- Dahlin, K., Mager, E.M., Allen, L., Tigue, Z., Goodglick, L., Wadehra, M., and Dobbs, L. (2004). Identification of genes differentially expressed in rat alveolar type I cells. *Am. J. Respir. Cell Mol. Biol.* 31, 309–316.
- Dai, Y., Jablons, D., and You, L. (2017). Hippo pathway in lung development. *J. Thorac. Dis.* 9, 2246–2250.
- Demling, N., Ehrhardt, C., Kasper, M., Laue, M., Knels, L., and Rieber, E.P. (2006). Promotion of cell adherence and spreading: A novel function of RAGE, the highly selective differentiation marker of human alveolar epithelial type I cells. *Cell Tissue Res.* 323, 475–488.
- Deng, F., Peng, L., Li, Z., Tan, G., Liang, E., Chen, S., Zhao, X., and Zhi, F. (2018). YAP triggers the Wnt/beta-catenin signalling pathway and promotes enterocyte self-renewal, regeneration and tumorigenesis after DSS-induced injury. *Cell Death Dis* 9, 153.
- Denny, S.K., Yang, D., Chuang, C.H., Brady, J.J., Lim, J.S., Gruner, B.M., Chiou, S.H., Schep, A.N., Baral, J., Hamard, C., et al. (2016). Nfib promotes metastasis through a widespread increase in chromatin accessibility. *Cell* 166, 328–342.
- Du, Y., Guo, M., Whitsett, J.A., and Xu, Y. (2015). 'LungGENS': A web-based tool for mapping single-cell gene expression in the developing lung. *Thorax* 70, 1092–1094.
- Frank, D.B., Peng, T., Zepp, J.A., Snitow, M., Vincent, T.L., Penkala, I.J., Cui, Z., Herriges, M.J., Morley, M.P., Zhou, S., et al. (2016). Emergence of a wave of Wnt signaling that regulates lung alveologenesis by controlling epithelial self-renewal and differentiation. *Cell Rep.* 17, 2312–2325.
- Frank, D.B., Penkala, I.J., Zepp, J.A., Sivakumar, A., Linares-Saldana, R., Zacharias, W.J., Stolz, K.G., Pankin, J., Lu, M., Wang, Q., et al. (2019). Early lineage specification defines alveolar

epithelial ontogeny in the murine lung. *Proc. Natl. Acad. Sci. U S A.* 116, 4362–4371.

Gokey, J.J., Sridharan, A., Xu, Y., Green, J., Carraro, G., Stripp, B.R., Perl, A.T., and Whitsett, J.A. (2018). Active epithelial Hippo signaling in idiopathic pulmonary fibrosis. *JCI Insight* 3, e98738.

Grant, C.E., Bailey, T.L., and Noble, W.S. (2011). FIMO: Scanning for occurrences of a given motif. *Bioinformatics* 27, 1017–1018.

Guo, M., Du, Y., Gokey, J.J., Ray, S., Bell, S.M., Adam, M., Sudha, P., Perl, A.K., Deshmukh, H., Potter, S.S., et al. (2019). Single cell RNA analysis identifies cellular heterogeneity and adaptive responses of the lung at birth. *Nat. Commun.* 10, 37.

Guo, M., Wang, H., Potter, S.S., Whitsett, J.A., and Xu, Y. (2015). SINCERA: A pipeline for single-cell RNA-seq profiling analysis. *Plos Comput. Biol.* 11, e1004575. <https://doi.org/10.1371/journal.pcbi.1004575>.

Hogan, B.L., Barkauskas, C.E., Chapman, H.A., Epstein, J.A., Jain, R., Hsia, C.C., Niklason, L., Calle, E., Le, A., Randell, S.H., et al. (2014). Repair and regeneration of the respiratory system: Complexity, plasticity, and mechanisms of lung stem cell function. *Cell Stem Cell* 15, 123–138.

Hsu, Y.C., Osinski, J., Campbell, C.E., Litwack, E.D., Wang, D., Liu, S., Bachurski, C.J., and Gronostajski, R.M. (2011). Mesenchymal nuclear factor I B regulates cell proliferation and epithelial differentiation during lung maturation. *Dev. Biol.* 354, 242–252.

Isago, H., Mitani, A., Mikami, Y., Horie, M., Urushiyama, H., Hamamoto, R., Terasaki, Y., and Nagase, T. (2020). Epithelial expression of YAP and TAZ is sequentially required in lung development. *Am. J. Respir. Cell Mol. Biol.* 62, 256–266.

Karolchik, D., Hinrichs, A.S., Furey, T.S., Roskin, K.M., Sugnet, C.W., Haussler, D., and Kent, W.J. (2004). The UCSC table browser data retrieval tool. *Nucleic Acids Res.* 32, D493–D496.

Kasper, M., Haroske, G., and Muller, M. (1994). Species differences in lectin binding to pulmonary cells: Soybean agglutinin (SBA) as a marker of type I alveolar epithelial cells and alveolar macrophages in mini pigs. *Acta Histochem.* 96, 63–73.

Lacanna, R., Liccardo, D., Zhang, P., Tragesser, L., Wang, Y., Cao, T., Chapman, H.A., Morrisey, E.E., Shen, H., Koch, W.J., et al. (2019). Yap/Taz regulate alveolar regeneration and resolution of lung inflammation. *J. Clin. Invest.* 129, 2107–2122.

Lange, A.W., Sridharan, A., Xu, Y., Stripp, B.R., Perl, A.K., and Whitsett, J.A. (2015). Hippo/Yap signaling controls epithelial progenitor cell proliferation and differentiation in the embryonic and adult lung. *J. Mol. Cell Biol.* 7, 35–47.

Langmead, B., and Salzberg, S.L. (2012). Fast gapped-read alignment with Bowtie 2. *Nat. Methods* 9, 357–359.

Lechner, A.J., Driver, I.H., Lee, J., Conroy, C.M., Nagle, A., Locksley, R.M., and Rock, J.R. (2017). Recruited monocytes and type 2 Immunity

promote lung regeneration following pneumonectomy. *Cell Stem Cell* 21, 120–134 e7.

Lee, J., Reddy, R., Barsky, L., Weinberg, K., and Driscoll, B. (2006). Contribution of proliferation and DNA damage repair to alveolar epithelial type 2 cell recovery from hypoxia. *Am. J. Physiol. Lung Cell Mol. Physiol.* 290, L685–L694.

Lee, J.H., Kim, J., Gludish, D., Roach, R.R., Saunders, A.H., Barrios, J., Woo, A.J., Chen, H., Conner, D.A., Fujiwara, Y., et al. (2013). Surfactant protein-C chromatin-bound green fluorescence protein reporter mice reveal heterogeneity of surfactant protein C-expressing lung cells. *Am. J. Respir. Cell Mol. Biol.* 48, 288–298.

Little, D.R., Gerner-Mauro, K.N., Flodby, P., Crandall, E.D., Borok, Z., Akiyama, H., Kimura, S., Ostrin, E.J., and Chen, J. (2019). Transcriptional control of lung alveolar type 1 cell development and maintenance by NK homeobox 2-1. *Proc. Natl. Acad. Sci. U S A.* 116, 20545–20555.

Little, D.R., Lynch, A.M., Yan, Y., Akiyama, H., Kimura, S., and Chen, J. (2021). Differential chromatin binding of the lung lineage transcription factor NKX2-1 resolves opposing murine alveolar cell fates in vivo. *Nat. Commun.* 12, 2509.

Liu, F., Lagares, D., Choi, K.M., Stopfer, L., Marinkovic, A., Vrbanc, V., Probst, C.K., Hiemer, S.E., Sisson, T.H., Horowitz, J.C., et al. (2015). Mechanosignaling through YAP and TAZ drives fibroblast activation and fibrosis. *Am. J. Physiol. Lung Cell Mol. Physiol.* 308, L344–L357.

Lu, L., Li, Y., Kim, S.M., Bossuyt, W., Liu, P., Qiu, Q., Wang, Y., Halder, G., Finegold, M.J., Lee, J.S., and Johnson, R.L. (2010). Hippo signaling is a potent in vivo growth and tumor suppressor pathway in the mammalian liver. *Proc. Natl. Acad. Sci. U S A.* 107, 1437–1442.

Maeda, Y., Hunter, T.C., Loudy, D.E., Dave, V., Schreiber, V., and Whitsett, J.A. (2006). PARP-2 interacts with TTF-1 and regulates expression of surfactant protein-B. *J. Biol. Chem.* 281, 9600–9606.

Mahoney, J.E., Mori, M., Szymaniak, A.D., Varelas, X., and Cardoso, W.V. (2014). The hippo pathway effector Yap controls patterning and differentiation of airway epithelial progenitors. *Dev. Cell* 30, 137–150.

Matsuzaki, Y., Besnard, V., Clark, J.C., Xu, Y., Wert, S.E., Ikegami, M., and Whitsett, J.A. (2008). STAT3 regulates ABCA3 expression and influences lamellar body formation in alveolar type II cells. *Am. J. Respir. Cell Mol. Biol.* 38, 551–558.

Mitani, A., Nagase, T., Fukuchi, K., Aburatani, H., Makita, R., and Kurihara, H. (2009). Transcriptional coactivator with PDZ-binding motif is essential for normal alveolarization in mice. *Am. J. Respir. Crit. Care Med.* 180, 326–338.

Nabhan, A.N., Brownfield, D.G., Harbury, P.B., krasnow, M.A., and Desai, T.J. (2018). Single-cell Wnt signaling niches maintain stemness of alveolar type 2 cells. *Science* 359, 1118–1123.

Nantie, L.B., Young, R.E., Paltzer, W.G., Zhang, Y., Johnson, R.L., Verheyden, J.M., and Sun, X. (2018). Lats1/2 inactivation reveals Hippo function in alveolar type I cell differentiation during lung

transition to air breathing. *Development* 145, dev163105. <https://doi.org/10.1242/dev.163105>.

Otsubo, K., Goto, H., Nishio, M., Kawamura, K., Yanagi, S., Nishie, W., Sasaki, T., Maehama, T., Nishina, H., Mimori, K., et al. (2017). MOB1-YAP1/TAZ-NKX2.1 axis controls bronchioalveolar cell differentiation, adhesion and tumour formation. *Oncogene* 36, 4201–4211.

Ou, J., Liu, H., Yu, J., Kelliher, M.A., Castilla, L.H., Lawson, N.D., and Zhu, L.J. (2018). ATACseqQC: A bioconductor package for post-alignment quality assessment of ATAC-seq data. *BMC Genomics* 19, 169.

Pajtlar, K.W., Wei, Y., Okonechnikov, K., Silva, P.B.G., Vouri, M., Zhang, L., Brabetz, S., Sieber, L., Gully, M., Mauermann, M., et al. (2019). YAP1 subgroup supratentorial ependymoma requires TEAD and nuclear factor I-mediated transcriptional programmes for tumorigenesis. *Nat. Commun.* 10, 3914.

Park, H.W., Kim, Y.C., Yu, B., Moroishi, T., Mo, J.S., Plouffe, S.W., Meng, Z., Lin, K.C., Yu, F.X., Alexander, C.M., et al. (2015). Alternative Wnt signaling activates YAP/TAZ. *Cell* 162, 780–794.

Park, K.S., Whitsett, J.A., diPalma, T., Hong, J.H., Yaffe, M.B., and Zannini, M. (2004). TAZ interacts with TTF-1 and regulates expression of surfactant protein-C. *J. Biol. Chem.* 279, 17384–17390.

Penkala, I.J., Liberti, D.C., Pankin, J., Sivakumar, A., Kremp, M.M., Jayachandran, S., Katzen, J., Leach, J.P., Windmueller, R., Stolz, K., et al. (2021). Age-dependent alveolar epithelial plasticity orchestrates lung homeostasis and regeneration. *Cell Stem Cell.* S1934-5909(21)00184-3. <https://doi.org/10.1016/j.stem.2021.04.026>.

Perl, A.K., Wert, S.E., Nagy, A., Lobe, C.G., and Whitsett, J.A. (2002). Early restriction of peripheral and proximal cell lineages during formation of the lung. *Proc. Natl. Acad. Sci. U S A.* 99, 10482–10487.

Pfleger, C.M. (2017). The Hippo pathway: A master regulatory network important in development and dysregulated in disease. *Curr. Top. Dev. Biol.* 123, 181–228.

Piersma, B., Bank, R.A., and Boersema, M. (2015). Signaling in fibrosis: TGF-beta, WNT, and YAP/TAZ converge. *Front. Med. (Lausanne)* 2, 59.

Ramirez, R.D., Sheridan, S., Girard, L., Sato, M., Kim, Y., Pollack, J., Peyton, M., Zou, Y., Kurie, J.M., Dimaio, J.M., et al. (2004). Immortalization of human bronchial epithelial cells in the absence of viral oncoproteins. *Cancer Res.* 64, 9027–9034.

Rawlins, E.L., Ostrowski, L.E., Randell, S.H., and Hogan, B.L. (2007). Lung development and repair: Contribution of the ciliated lineage. *Proc. Natl. Acad. Sci. U S A.* 104, 410–417.

Reynolds, S.D., Reynolds, P.R., Pryhuber, G.S., Finder, J.D., and Stripp, B.R. (2002). Secretoglobins SCGB3A1 and SCGB3A2 define secretory cell subsets in mouse and human airways. *Am. J. Respir. Crit. Care Med.* 166, 1498–1509.

Rock, J.R., Barkauskas, C.E., Cronic, M.J., Xue, Y., Harris, J.R., Liang, J., Noble, P.W., and Hogan, B.L. (2011). Multiple stromal populations contribute to pulmonary fibrosis without

evidence for epithelial to mesenchymal transition. *Proc. Natl. Acad. Sci. U S A.* 108, E1475–E1483.

Rock, J.R., Randell, S.H., and Hogan, B.L. (2010). Airway basal stem cells: A perspective on their roles in epithelial homeostasis and remodeling. *Dis. Model Mech.* 3, 545–556.

Rockich, B.E., Hrycaj, S.M., Shih, H.P., Nagy, M.S., Ferguson, M.A., Kopp, J.L., Sander, M., Wellik, D.M., and Spence, J.R. (2013). Sox9 plays multiple roles in the lung epithelium during branching morphogenesis. *Proc. Natl. Acad. Sci. U S A.* 110, E4456–E4464.

Simon, R., Lam, A., Li, M.C., Ngan, M., Meneses, S., and Zhao, Y. (2007). Analysis of gene expression data using BRB-ArrayTools. *Cancer Inform.* 3, 11–17.

Stein, C., Bardet, A.F., Roma, G., Bergling, S., Clay, I., Ruchti, A., Agarinis, C., Schmelzle, T., Bouwmeester, T., Schubeler, D., and Bauer, A. (2015). YAP1 exerts its transcriptional control via TEAD-mediated activation of enhancers. *Plos Genet.* 11, e1005465.

Trapnell, C., Williams, B.A., Pertea, G., Mortazavi, A., Kwan, G., van Baren, M.J., Salzberg, S.L., Wold, B.J., and Pachter, L. (2010). Transcript assembly and quantification by RNA-Seq reveals unannotated transcripts and isoform switching during cell differentiation. *Nat. Biotechnol.* 28, 511–515.

Treutlein, B., Brownfield, D.G., Wu, A.R., Neff, N.F., Mantalas, G.L., Espinoza, F.H., Desai, T.J., Krasnow, M.A., and Quake, S.R. (2014). Reconstructing lineage hierarchies of the distal lung epithelium using single-cell RNA-seq. *Nature* 509, 371–375.

Tsao, P.N., Vasconcelos, M., Izvolsky, K.I., Qian, J., Lu, J., and Cardoso, W.V. (2009). Notch signaling controls the balance of ciliated and secretory cell fates in developing airways. *Development* 136, 2297–2307.

Ustiyani, V., Zhang, Y., Perl, A.K., Whitsett, J.A., Kalin, T.V., and Kalinichenko, V.V. (2016). beta-catenin and Kras/Foxm1 signaling pathway are critical to restrict Sox9 in basal cells during pulmonary branching morphogenesis. *Dev. Dyn.* 245, 590–604.

van Soldt, B.J., and Cardoso, W.V. (2020). Hippo-Yap/Taz signaling: Complex network interactions and impact in epithelial cell behavior. *Wiley Interdiscip. Rev. Dev. Biol.* 9, e371. <https://doi.org/10.1002/wdev.371>.

van Soldt, B.J., Qian, J., Li, J., Tang, N., Lu, J., and Cardoso, W.V. (2019). Yap and its subcellular localization have distinct compartment-specific roles in the developing lung. *Development* 146, dev175810. <https://doi.org/10.1242/dev.175810>.

Varelas, X. (2014). The Hippo pathway effectors TAZ and YAP in development, homeostasis and disease. *Development* 141, 1614–1626.

Vaughan, A.E., Brumwell, A.N., Xi, Y., Gotts, J.E., Brownfield, D.G., Treutlein, B., Tan, K., Tan, V., Liu, F.C., Looney, M.R., et al. (2015). Lineage-negative progenitors mobilize to regenerate lung epithelium after major injury. *Nature* 517, 621–625.

Vaughan, A.E., and Chapman, H.A. (2013). Regenerative activity of the lung after epithelial injury. *Biochim. Biophys. Acta* 1832, 922–930.

Wan, H., Luo, F., Wert, S.E., Zhang, L., Xu, Y., Ikegami, M., Maeda, Y., Bell, S.M., and Whitsett, J.A. (2008). Kruppel-like factor 5 is required for perinatal lung morphogenesis and function. *Development* 135, 2563–2572.

Wang, Z., Shu, W., Lu, M.M., and Morrissey, E.E. (2005). Wnt7b activates canonical signaling in epithelial and vascular smooth muscle cells through interactions with Fzd1, Fzd10, and LRP5. *Mol. Cell Biol.* 25, 5022–5030.

Wang, Z., Ye, J., Deng, Y., Yan, Z., Denduluri, S., and He, T.C. (2014). Wnt versus Hippo: A balanced act or dynamic duo? *Genes Dis.* 1, 127–128.

Warburton, D., Tefft, D., Mailloux, A., Bellusci, S., Thiery, J.P., Zhao, J., Buckley, S., Shi, W., and Driscoll, B. (2001). Do lung remodeling, repair, and regeneration recapitulate respiratory ontogeny? *Am. J. Respir. Crit. Care Med.* 164, S59–S62.

Wert, S.E., Dey, C.R., Blair, P.A., Kimura, S., and Whitsett, J.A. (2002). Increased expression of thyroid transcription factor-1 (TTF-1) in respiratory epithelial cells inhibits alveolarization and causes pulmonary inflammation. *Dev. Biol.* 242, 75–87.

Whitsett, J.A., Kalin, T.V., Xu, Y., and Kalinichenko, V.V. (2019). Building and regenerating the lung cell by cell. *Physiol. Rev.* 99, 513–554.

Xu, Y., Mizuno, T., Sridharan, A., Du, Y., Guo, M., Tang, J., Wikenheiser-Brokamp, K.A., Perl, A.T., Funari, V.A., Gokey, J.J., et al. (2016). Single-cell RNA sequencing identifies diverse roles of epithelial cells in idiopathic pulmonary fibrosis.

*JCI Insight* 1, e90558. <https://doi.org/10.1172/jci.insight.90558>.

Yu, F.X., Zhao, B., and Guan, K.L. (2015). Hippo pathway in organ size control, tissue homeostasis, and cancer. *Cell* 163, 811–828.

Zacharias, W.J., Frank, D.B., Zepp, J.A., Morley, M.P., Alkhaleel, F.A., Kong, J., Zhou, S., Cantu, E., and Morrissey, E.E. (2018). Regeneration of the lung alveolus by an evolutionarily conserved epithelial progenitor. *Nature* 555, 251–255.

Zepp, J.A., Zacharias, W.J., Frank, D.B., Cavanaugh, C.A., Zhou, S., Morley, M.P., and Morrissey, E.E. (2017). Distinct mesenchymal lineages and niches promote epithelial self-renewal and myofibrogenesis in the lung. *Cell* 170, 1134–1148 e10.

Zhang, N., Bai, H., David, K.K., Dong, J., Zheng, Y., Cai, J., Giovannini, M., Liu, P., Anders, R.A., and PAN, D. (2010). The Merlin/NF2 tumor suppressor functions through the YAP oncoprotein to regulate tissue homeostasis in mammals. *Dev. Cell* 19, 27–38.

Zhao, B., Tumaneng, K., and Guan, K.L. (2011). The Hippo pathway in organ size control, tissue regeneration and stem cell self-renewal. *Nat. Cell Biol.* 13, 877–883.

Zhao, B., Wei, X., Li, W., Udan, R.S., Yang, Q., Kim, J., Xie, J., Ikenoue, T., Yu, J., Li, L., et al. (2007). Inactivation of YAP oncoprotein by the Hippo pathway is involved in cell contact inhibition and tissue growth control. *Genes Dev.* 21, 2747–2761.

Zhao, C., Li, Y., Qiu, W., He, F., Zhang, W., Zhao, D., Zhang, Z., Zhang, E., Ma, P., Liu, Y., et al. (2018). C5a induces A549 cell proliferation of non-small cell lung cancer via GDF15 gene activation mediated by GCN5-dependent KLF5 acetylation. *Oncogene* 37, 4821–4837.

Zhao, R., Fallon, T.R., Saladi, S.V., Pardo-Saganta, A., Villoria, J., Mou, H., Vinarsky, V., Gonzalez-Celeiro, M., Nunna, N., Hariri, L.P., et al. (2014). Yap tunes airway epithelial size and architecture by regulating the identity, maintenance, and self-renewal of stem cells. *Dev. Cell* 30, 151–165.

Zhi, X., Zhao, D., Zhou, Z., Liu, R., and Chen, C. (2012). YAP promotes breast cell proliferation and survival partially through stabilizing the KLF5 transcription factor. *Am. J. Pathol.* 180, 2452–2461.

Zuo, W., Zhang, T., Wu, D.Z., Guan, S.P., Liew, A.A., Yamamoto, Y., Wang, X., Lim, S.J., Vincent, M., Lessard, M., et al. (2015). p63(+)Krt5(+) distal airway stem cells are essential for lung regeneration. *Nature* 517, 616–620.

STAR★METHODS

KEY RESOURCES TABLE

REAGENT or RESOURCE	SOURCE	IDENTIFIER
<i>Antibodies</i>		
YAP	Seven Hills Bioreagents	WRAB
SFTPC	Seven Hills Bioreagents	N/A
SFTPC	Seven Hills Bioreagents	1231: RRID:AB_451721
SFTPC	Santa Cruz	SC-7706:RRID:AB_2185507
HOPX	Santa Cruz	SC-398703:RRID:AB_2687966
AGER	R&D systems	AF1145:RRID:AB_354628
NKX2-1	Seven Hills Bioreagents	1231:RRID:AB_2832953
NKX2-1	Seven Hills Bioreagents	N/A
SFTPB	Seven Hills Bioreagents	GP20
KI67	BD Biosciences	556003:RRID:AB_396287
SOX9	Millipore	AB-5535: RRID:AB_2239761
KLF5	Seven Hills Bioreagents	N/A
NFIB	Novus Bio	NBP1-81000:RRID:AB_11027763
MUC5B	Santa Cruz	SC-20119:RRID:AB_2282256
SCGB1A1	Seven Hills Bioreagents	N/A
FOXF1	R&D systems	AF 4798:RRID:AB_2105588
FLAG	Cell Signaling	8146s:RRID:AB_10950495
FLAG	Cell Signaling	14793S:RRID:AB_2572291
HA	Cell Signaling	2362s:RRID:AB_2890916
<i>Deposited data</i>		
Yap_active_Atac1	GSE154527	GSM4672910
Yap_active_Atac2	GSE154527	GSM4672911
Yap_active_Atac3	GSE154527	GSM4672912
Yap_active_control_Atac1	GSE154527	GSM4672913
Yap_active_control_Atac2	GSE154527	GSM4672914
Yap_active_control_Atac3	GSE154527	GSM4672915
Yap_active_control_RNAseq1	GSE154527	GSM4672916
Yap_active_control_RNAseq2	GSE154527	GSM4672917
Yap_active_control_RNAseq3	GSE154527	GSM4672918
Yap_active_control_RNAseq4	GSE154527	GSM4672919
Yap_active_RNAseq1	GSE154527	GSM4672920
Yap_active_RNAseq2	GSE154527	GSM4672921
Yap_active_RNAseq3	GSE154527	GSM4672922
Yap_active_RNAseq4	GSE154527	GSM4672923
Yap_active_RNAseq5	GSE154527	GSM4672924
Yap_active_RNAseq6	GSE154527	GSM4672925
Yap_deleted_Atac1	GSE154527	GSM4672926
Yap_deleted_Atac2	GSE154527	GSM4672927
Yap_deleted_control_Atac1	GSE154527	GSM4672928
Yap_deleted_control_RNAseq1	GSE154527	GSM4672929

(Continued on next page)

**Continued**

REAGENT or RESOURCE	SOURCE	IDENTIFIER
Yap_deleted_control_RNAseq2	GSE154527	GSM4672930
Yap_deleted_control_RNAseq3	GSE154527	GSM4672931
Yap_deleted_control_RNAseq4	GSE154527	GSM4672932
Yap_deleted_RNAseq1	GSE154527	GSM4672933
Yap_deleted_RNAseq2	GSE154527	GSM4672934
Yap_deleted_RNAseq3	GSE154527	GSM4672935
Yap_deleted_RNAseq4	GSE154527	GSM4672936
Yap_deleted_RNAseq5	GSE154527	GSM4672937

Experimental models: cell lines

HBEC3KT	Dr. John D. Minna	Multiple repositories: RRID:CVCL_X491
---------	-------------------	--

Experimental models: organisms/strains

<i>Sftpc</i> <sup>tm1(cre/ERT2)Blh</sup> <i>Stk3</i> <sup>fl/fl</sup> / <i>Stk4</i> <sup>fl/fl</sup>	Generated through crossing below lines in house	Requestable
<i>Sftpc</i> <sup>tm1(cre/ERT2)Blh</sup> <i>Yap</i> <sup>fl/fl</sup>	Generated through crossing below lines in house	Requestable
<i>Sftpc</i> <sup>tm1(cre/ERT2)Blh</sup>	Dr. Brigid Hogan, now available at The Jackson Laboratory	028054: RRID:IMSR_JAX:028054
<i>Stk3</i> <sup>fl/fl</sup> / <i>Stk4</i> <sup>fl/fl</sup>	Dr. Randy L. Johnson/ The Jackson Laboratory	017635: RRID:IMSR_JAX:017635
<i>Yap</i> <sup>fl/fl</sup>	The Jackson Laboratory	027929: RRID:IMSR_JAX:027929

Oligonucleotides

YAP1	ThermoFisher	Hs00902712_g1
KLF5	ThermoFisher	Hs00156145_m1
AGER	ThermoFisher	Hs00542584_g1
<i>Yap1</i>	ThermoFisher	Mm01143263_m1
<i>Klf5</i>	ThermoFisher	Mm00456521_m1
<i>Nfib</i>	ThermoFisher	Mm01257777_m1
18S	ThermoFisher	4352930E
<i>Nkx2-1</i>	ThermoFisher	Mm00447558_m1
<i>Ajuba</i>	ThermoFisher	Mm00495049_m1
<i>Ctgf</i>	ThermoFisher	Mm01192933_g1
<i>Stk4</i>	ThermoFisher	Mm00490480_m1
<i>Stk3</i>	ThermoFisher	Mm00451755_m1
<i>Ager</i>	ThermoFisher	Mm01134790_g1
<i>Aqp5</i>	ThermoFisher	Mm00437578_m1
<i>Elf3</i>	ThermoFisher	Mm01295975_m1
<i>Muc5b</i>	ThermoFisher	Mm00466391_m1
<i>Scgb1a1</i>	ThermoFisher	Mm00442046_m1
<i>Scgb3a1</i>	ThermoFisher	Mm00446493_m1
<i>Scgb3a2</i>	ThermoFisher	Mm00504412_m1

Recombinant DNA

pCAGG:NFB2:HA	Addgene	112700:RRID:Addgene_112700
pCDNA:KLF5	Reference # 54	Requestable

(Continued on next page)

**Continued**

REAGENT or RESOURCE	SOURCE	IDENTIFIER
pCMV-flag (S127A)YAP	Addgene	27370: RRID:Addgene_27370
pCDNA:NKX2-1	Reference # 79	Requestable
pGL3:KLF5:Luciferase	Reference # 54	Requestable
pLenti:AGER:Luciferase	ABM	C449
pLenti:AGER NKX2-1Δ:Luciferase	ABM	C047
pLenti:AGER NFIBΔ:Luciferase	ABM	C047
pLenti:AGER TEADΔ:Luciferase	ABM	C047

**RESOURCE AVAILABILITY**

**Lead contact**

Request for further information, resources and reagents should be directed to the lead contact Jason J. Gokey ([Jason.j.gokey@vumc.org](mailto:Jason.j.gokey@vumc.org)) by which request will be fulfilled.

**Materials availability**

All plasmids and mice within this study were acquired as per the following method section details. Request for further information should be directed to the lead contact.

**Additional information**

Any additional information required to reanalyze the data reported in this paper is available from the lead contact upon request.

**Data and code availability**

RNA-seq and ATAC-seq data generated in this study are available through GEO, GSE 154527. See [key resources table](#) for additional accession information. This paper does not report original code. Requests of any data reported in this paper will be shared by the lead contact upon request.

**EXPERIMENTAL MODEL AND SUBJECT DETAILS**

Mice were housed and bred in accordance with protocols approved by the IACUC of Cincinnati Children's Research Foundation. To generate AT2 cell-specific activation or deletion of YAP, *Sftpc*<sup>tm1(cre/ERT2)Blh</sup> heterozygous mice (a kind gift from Dr. Brigid Hogan) (Rock et al., 2011) were crossed with *Stk3*<sup>fllox/fllox</sup>*Stk4*<sup>fllox/fllox</sup> (Lu et al., 2010) or *Yap*<sup>fllox/fllox</sup> mice (Zhang et al., 2010). *SftpcCre*<sup>ert2</sup> heterozygous and WT mouse pups were treated with tamoxifen at PND3. *SftpcCre*<sup>ert2</sup>*Stk3*<sup>fllox/fllox</sup>*Stk4*<sup>fllox/fllox</sup> or *SftpcCre*<sup>ert2</sup>*Yap*<sup>fllox/fllox</sup> were considered experimental mice and *Stk3*<sup>fllox/fllox</sup>*Stk4*<sup>fllox/fllox</sup> or *Yap*<sup>fllox/fllox</sup> mice were used as tamoxifen injected WT littermate controls. All mice used for this study were not previously used for other procedures and were not used as breeding mice prior to study. Mice used throughout the project are listed as follows: Genotype, age sacrificed, and sex as N = male (female). *Yap*<sup>fllox/fllox</sup> PND14 N = 9(10), *SftpcCre*<sup>ert2</sup>*Yap*<sup>fllox/fllox</sup> PND14 N = 15(14), *Stk3*<sup>fllox/fllox</sup>*Stk4*<sup>fllox/fllox</sup> PND14 N = 10(11), *SftpcCre*<sup>ert2</sup>*Stk3*<sup>fllox/fllox</sup>*Stk4*<sup>fllox/fllox</sup> PND14 N = 16(15). *Yap*<sup>fllox/fllox</sup> PND28 N = 2(2), *SftpcCre*<sup>ert2</sup>*Yap*<sup>fllox/fllox</sup> PND28 N = 4(4), *Stk3*<sup>fllox/fllox</sup>*Stk4*<sup>fllox/fllox</sup> PND28 N = 3(2), *SftpcCre*<sup>ert2</sup>*Stk3*<sup>fllox/fllox</sup> PND28 N = 4(5). *Yap*<sup>fllox/fllox</sup> PND90 N = 2(2), *SftpcCre*<sup>ert2</sup>*Yap*<sup>fllox/fllox</sup> PND90 N = 4(4), *Stk3*<sup>fllox/fllox</sup>*Stk4*<sup>fllox/fllox</sup> PND90 N = 2(2), *SftpcCre*<sup>ert2</sup>*Stk3*<sup>fllox/fllox</sup>*Stk4*<sup>fllox/fllox</sup> PND14 N = 4(4).

**METHOD DETAILS**

**Immunofluorescence analysis**

Mouse lungs were fixed in 4% PFA overnight and embedded in paraffin. Lung tissue sections (7μm) were deparaffinized and blocked in a 4% normal donkey serum in Phosphate Buffered Saline-0.1% Triton X-100 (PBST) (blocking agent) for 1 hr. Primary antibodies were diluted in blocking agent and incubated

at 4°C overnight. Samples were washed three times in PBST and incubated in 1:200 dilution fluorescently conjugated secondary antibody for 1 hr at room temperature. Samples were washed three times in PBST, counterstained with DAPI for 15 min, washed in PBST three times and mounted in ProLong Gold (ThermoFisher) antifade mounting media. Confocal imaging was performed on a Nikon A1R LUNV inverted confocal microscope at 20X and 60X magnification. Image analysis was performed using Nikon Elements software to count cell numbers and analyze alveolar space. RNAScope and YAP+ AT2 cell quantification imaging was acquired using a Keyence BZ-X710 with BZ-X Viewer software with a 40X objective. Image analysis was performed with automated HALO image analysis software. The total number of DAPI-positive and YAP-positive nuclei were quantified. To assess AT2 cell number, DAPI-positive nuclei having SFTPC were quantified using the HALO cell segmentation software feature, and AT2 cells having YAP-positive nuclei were quantified to identify the number of YAP active AT2 cells.

### RNAScope

RNAScope technology (ACDBio) was used to perform fluorescent RNA *in situ* hybridization (RNA ISH) experiments according to manufacturer's instructions. RNAScope probes against *Sftpc* (314101-C4), *Scgb1a1* (420351-C3), and *Muc5b* (47991) were used.

### Alveolar epithelial cell enrichment

Whole mouse lungs were incubated in dispase followed by addition of DNase and dissociation using a gentleMACS. Cells were centrifuged, resuspended in DMEM and passed through a 40µm filter to obtain single cell suspensions from the whole lung. AT2 cells were isolated using MACs magnetic bead (Miltenyi Biotec) with negative selection of CD45 (BioLegend), CD16/32 (Fisher), Ter119 (BioLegend), CD90.2 (BioLegend), CD271 (Miltenyi Biotec), and CD31 (BioLegend) (Corti et al., 1996), followed by positive selection of CD326 (Miltenyi Biotec). Due to subsequent identification of AT2 cells expressing markers associated with other epithelial cell types in YAP<sup>active</sup> and YAP<sup>deleted</sup> mice, isolated AT2 cells are interchangeably referred to as "EPCAM+ cells".

### Organoid culture

Organoids were produced by combining 5000 AT2 cells with 50,000 fibroblasts (isolated from PND14 wild type C57Bl6 mice and cultured for 3 passages). Cells were mixed in a 1:1 ratio with Matrigel and plated in 24 well plate transwell inserts. Cells were cultured for the first 24 hr with SAGM (Lonza) + Rock inhibitor (Y27632 Sigma), and subsequently cultured in SAGM without Rock inhibitor for 21 days. Organoids were then fixed in 4% PFA overnight, paraffin embedded, and processed for histological analysis. Brightfield images of organoid wells are available in [Figure S1M](#).

### Cell culture and transfections

HBEC3-KT (referred to as HBEC3) human bronchial epithelial cells were a kind gift from Dr John D. Minna (UT Southwestern) (Ramirez et al., 2004). HBEC3 cells were plated at  $1.2 \times 10^5$  cells per well in 12-well culture plates and cultured in KFSM (Gibco, ThermoFisher). Cells were transfected at 50-60% confluence with plasmid DNA and Fugene HD (Promega) according to manufacturer's instructions. Plasmids used were acquired as follows: pCAGG:NFB2:HA (112700 Addgene), pCDNA:KLF5 (Wan et al., 2008), pCMV-flag (S127A)YAP (27370 Addgene) (Zhao et al., 2007), pCDNA:NKX2-1 (Maeda et al., 2006), pGL3:KLF5:Luciferase, pLenti:AGER:Luciferase (ABM). Site-mutagenesis of 5 base pairs within respective predicted transcription factor binding sites was performed by ABM Inc., to obtain *Ager NKX2-1Δ*, *AGER TEADΔ*, and *AGER NFIBΔ* from the parent pLenti:AGER:Luciferase construct. Cells were lysed for assays 48 hr after transfection.

### Co-immunoprecipitation

HBEC3 cells were cultured at  $2.4 \times 10^5$  in 6 well plates and transfected with pCMV-flag (S127A)YAP and/or pCAGG:NFB-HA. Cells were lysed with 100µL of extraction buffer B as per Dynabeads protocol (ThermoFisher). Samples were split into 3 equal groups and 5% input was saved. Samples were incubated overnight at 4°C with magnetic beads conjugated to HA, FLAG, or mouse IgG and the bound fraction was separated using magnetic µ-columns and eluted per manufacturer's protocol (Miltenyi Biotec). Samples were separated on 10-20% Tris-glycine gradient gels (ThermoFisher) and transferred onto PVDF membranes (Millipore Sigma) using an iBlot Gel Transfer Device (ThermoFisher). Membranes were blocked with 5% milk/Tris Buffered Saline-0.1% Tween-20 (TBST) and incubated in primary antibody at 1:1000

overnight at 4°C. Blots were washed three times in TBST and incubated with TrueBlot HRP-conjugated secondary antibody at 1:1000 dilution (Rockland).

### Gene promoter assays

Gene promoter-luciferase reporter constructs were transfected at 0.5 µg/well with an empty vector and/or plasmid DNA expression constructs for transcription factor activators at ratios of 1:3, 1:10, or 1:24 activator:promoter DNA. Cells were harvested 48 hr after transfection by lysing with Luciferase Cell Culture Lysis 5X Reagent (Promega). Luciferase activity was assayed using the AutoLumat Plus (Berthold Technologies). Transfections were performed in triplicate and all experiments were repeated multiple times to generate  $N > 9$  for all assays.

### RNA analysis

RNA was extracted from HBEC3 cells using the RNeasy Micro kit (Qiagen) according to manufacturer's instructions with an on-column DNase I digestion step. RNA was extracted from isolated mouse EPCAM+ cells using an RNeasy Mini kit (Qiagen) with on-column DNase I digestion as per manufacturer's protocol. Sequencing was performed on RNA isolated from mouse EPCAM+ cells. RNA was reverse transcribed into cDNA (HBEC3 and isolated mouse EPCAM+ cells) using an iScript cDNA synthesis kit (Biorad). qRT-PCR assays were performed using either an Applied Biosystems Quantstudio 5 or a StepOne Plus Real-Time PCR System (ThermoFisher).

### ATAC-seq analysis

For ATAC-seq analysis,  $5 \times 10^4$  cells were used from purified EPCAM+ cells collected from WT, YAP<sup>active</sup> or YAP<sup>deleted</sup> mouse lungs. Remaining EPCAM+ cells from each mouse were used for RNA-seq. DNA fragments were isolated, barcoded, and sequenced following published protocols (Buenrostro et al., 2015). Sequencing was performed by Genewiz using an Illumina HiSeq 4000 with a 2X150bp sequencing strategy

### Bioinformatics

Paired-end ATAC-seq and RNA-seq analyses were performed on EPCAM+ cells isolated from PND14 YAP<sup>active</sup>, YAP<sup>deleted</sup> and WT mouse lungs. ATAC-seq FASTQ files were processed in Galaxy (Afgan et al., 2018). Reads were trimmed and adaptors removed by TrimGalore prior alignment to 10mm with Bowtie2 (Langmead and Salzberg, 2012). Mitochondrial DNA was removed by using BAM filter (Barnett et al., 2011) and duplicate reads or reads larger than 100bp were filtered out by Picard MarkDuplicates (<http://broadinstitute.github.io/picard>). For initial ATAC-seq peak identification, individual mutants were compared to their age-matched controls using Homer (1v1,  $p < .01$ ,  $FC > 2$ , YAP<sup>deleted</sup>  $N = 2$ , YAP<sup>flox/flox</sup>  $N = 1$ , YAP<sup>active</sup>  $N = 2$ , Stk3<sup>flox/flox</sup>Stk4<sup>flox/flox</sup>  $N = 1$ ). Resulting replicate peak files were merged and annotated. YAP<sup>active</sup> ATAC- BAM files were further analyzed with Macs2 using broad peak detections and a  $p < .01$  cutoff. YAP<sup>active</sup> ( $N = 3$ ) were compared to WT (Stk3<sup>flox/flox</sup>Stk4<sup>flox/flox</sup>  $N = 3$ ) and litters were analyzed separately to create two differential peak files. Differential peak files were merged using Homer and only differential peaks present in both YAP<sup>active</sup> litters were kept. Peaks were then annotated by Homer and separated into peaks within gene promoters or other regulatory regions. Functional enrichment analysis was performed on genes with differentially opened peaks in their promoter regions. Homer's motif enrichment was performed on open promoter regions to determine enriched transcription factor binding sites. IGV viewer was used to visualize peaks and promoters. MACS2 was used to obtain total number of peaks, ATACseqQC (Ou et al., 2018) was used to calculate TSS enrichment score and bedtools intersect was used to calculate FRiP score. PCA analyses were done on ATAC-seq BAM files using DESeq and gene coding ATAC-seq. Differential peaks were visualized in a volcano plot.

RNA-seq FASTQ files generated from YAP<sup>active</sup> ( $N = 6$ ) and WT littermates ( $N = 4$ ) or YAP<sup>deleted</sup> ( $N = 5$ ) and WT littermates ( $N = 4$ ) were trimmed and adaptors were removed by TrimGalore. Trimmed FASTQ files were aligned and sorted by Bowtie2. Sorted BAM files were used to identify differentially expressed genes using DESeq and Fragments Per Kilobase of transcript per Million mapped reads (FPKM) values were calculated by Cufflinks (Trapnell et al., 2010). Differentially expressed genes were identified using a  $p < .01$ ,  $FC > 1.5$  and  $FPKM > 1$  in over half of the replicates in at least one condition being compared. Subsets of differentially expressed genes were analyzed by Toppfun's functional enrichment analyses to predict altered biological functions (Chen et al., 2009). Promoter regions 1.5kb upstream of the predicted transcriptional start site of genes induced in YAP<sup>active</sup> mice were analyzed using MEME suite's AME coupled with Meme

Suite's Motif database. Promoter sequences were downloaded using the UCSC Table browser (Karolchik et al., 2004). Select motif locations in DNA sequences of interest were identified using Meme suites Fimo package with  $p < 0.0005$  as cutoff (Grant et al., 2011). BRB was used for hierarchical clustering and dendrogram generation (Simon et al., 2007). RNA-seq analysis demonstrated background gene expression changes between  $Yap^{flox/flox}$  WT AT2 cells and  $Stk3^{flox/flox}/Stk4^{flox/flox}$  WT AT2 cells which prevented direct comparisons between control mice.

AT1 or AT2 specific transcriptional regulatory networks (TRNs) were predicted by analyzing Fluidigm C1 based single-cell RNA sequencing of E18.5 mouse lungs previously sequenced and analyzed (Bridges et al., 2020). To infer the TRNs, AT1 or AT2 specific differentially expressed genes were used as potential target genes and transcriptional factors commonly or selectively expressed in AT1 or AT2 were identified as potential transcription factor regulators. AT1 or AT2 specific target genes were defined as genes with a Welch's ttest  $p < 0.05$  and fold change  $> 1.5$  in AT1 or AT2 when compared to all the other cells. For a given cell type, transcription factors with cell type frequency  $> 70\%$  were considered as commonly expressed and transcription factors with either their first or second top expression value occurring in a cell type coupled with a cell type frequency  $> 40\%$  were identified as selectively expressed. Transcription factors or transcription cofactors were defined based on Genomatix (MatBase 9.1 of Genomatix), IPA (Qiagen) and CIS-BP. Significance of interactions between transcription factors and target genes in a cell type were assessed based on a first-order conditional dependence driving force prediction method we previously developed (Du et al., 2015). The predicted AT1 TRN was constructed with 353 nodes (104 TF's) and 2757 unique edges that passed the threshold ( $S_{ij} < 0.001$ ). The predicted AT2 TRN was constructed with 363 nodes (53 TF's) and 1353 unique edges that passed the threshold ( $S_{ij} < 0.001$ ). Transcription factors were ranked based on the importance of the node to the inferred AT1 or AT2 TRNs using a method combining the six node importance metrics (Degree Centrality, Closeness Centrality, Betweenness Centrality, Disruptive Fragmentation Centrality, Disruptive Connection Centrality and Disruptive Distance Centrality) as described in SINCERA (Du et al., 2015).

### Quantification and statistical analysis

Quantification and statistical analysis, outside the scope of RNA-seq and ATAC-seq bioinformatic analysis, was performed on GraphPad prism. For all N stated, N is equivalent to number of mice or experimental wells used for an experiment. For all multi-variate analysis, statistical significance was determined using Two-way ANOVA followed by Sidak's or Tukey's multiple comparison test. Single variant analysis was performed using Welch's t test. P-values deemed significant can be found in the figure legend of each figure along with the definition of what error bar and whiskers represent. No samples were excluded from respective analyses of each figure.